Formation Control for Agents Modeled with Extended Unicycle Dynamics that Includes Orientation Kinematics on SO(m) and Speed Constraints*

Christopher Heintz and Jesse B. Hoagg Department of Mechanical Engineering, The University of Kentucky, Lexington, KY 40506-0503¹

Abstract

We present a formation control algorithm for agents with extended unicycle dynamics that include orientation kinematics on SO(m), first-order uncertain speed dynamics, and hard constraints on speed. The desired interagent positions are expressed in a leader-fixed coordinate frame. Thus, the desired interagent positions vary in time as the leader-fixed frame rotates. We assume that each agent has relative-position feedback of its neighbor agents, where the neighbor sets are such that the interagent communication (i.e., feedback) structure is a quasi-strongly connected directed graph. We assume that at least one agent (which is a center vertex of the graph) has access to a measurement its position relative to the leader. The main analytic results show that for almost all initial conditions, each agent converges to its desired relative position with the leader and the other agents, and each agent's speed satisfies the speed constraints for all time. We also present an adaptive extension of the formation control algorithm that addresses uncertain speed dynamics, which are parameterized as an unknown linear combination of known basis functions. Finally, we present numerical simulations to demonstrate both the non-adaptive and adaptive formation control methods.

Keywords: Multi-agent systems, formation control, extended unicycle, state constraints

1. Introduction

Autonomous multi-vehicle systems have application to distributed sensing, cooperative surveillance, precision agriculture, and search and rescue. In formation control, each agent typically relies on sensing or interagent communication to determine necessary feedback information (e.g., interagent positions). Then, each agent uses this feedback information in combination with feedforward information (e.g., external commands, mission objectives) to accomplish tasks such as collision avoidance, cohesion, guidance, and velocity matching. Collision avoidance repels an agent from nearby agents or obstacles, whereas cohesion attracts an agent to nearby agents. Guidance often causes each agent to approach a desired destination [1, 2] or follow a leader agent [3–7]. Velocity matching causes nearby agents to approach a consensus velocity [8–10].

Consensus algorithms have been used to address cohesion (e.g., [5–7, 11, 12]). These approaches force agents into a predetermined formation by specifying the desired relative position between pairs of agents. Other examples of formation control algorithms include [1–3, 13–15]. Examples of formation control algorithms that address uncertain agent dynamics include [12, 16–18], whereas methods that address input saturation are presented in [6, 11, 19]. Surveys of multi-agent formation-control methods are presented in [9, 10, 20].

Much of the cooperative control literature (e.g., [1, 3, 7, 10–12, 14, 17, 21, 22]) focuses on agents with double-integrator dynamics, where the control input is the acceleration in an inertial frame. However, double-integrator dynamics are not suitable for modeling some vehicles such as fixed-wing aircraft or wheeled robots, which are subject to nonholonomic constraints [2, 23, 24].

This paper addresses agents with extended unicycle dynamics that include orientation kinematics on SO(m), first-order uncertain speed dynamics, and hard speed constraints. These extended unicycle dynamics

^{*}This work is supported in part by the National Science Foundation (CNS-1932105, OIA-1539070) and the National Aeronautics and Space Administration (NNX15AR69H) through the NASA Kentucky Space Grant.

¹C. Heintz and J. B. Hoagg are with the Department of Mechanical Engineering, University of Kentucky, Lexington, KY, USA. (e-mail: cmhe234@g.uky.edu, jesse.hoagg@uky.edu).

have application to modeling fixed-wing unmanned air vehicles (UAVs) and ground robots. For example, similar models are used for fixed-wing UAVs in [25-29] and for ground robots in [2, 6, 30, 31]. However, these related models do not include orientation kinematics on SO(m), hard speed constraints, or uncertainty in the speed dynamics—all of which can be important for many applications. For example, a fixed-wing UAV has hard speed constraints; namely, it must satisfy a minimum speed to maintain lift, and its operational capabilities impose a limit on maximum speed. Similarly, the speed dynamics of a fixed-wing UAV typically has uncertainty from a variety of sources, which could include local air density, airframe configuration, level of battery charge, and payload mass (e.g., remaining fuel, cargo). In addition, these parameters may change during flight. Thus, it may be beneficial to treat this as parameterized uncertainty rather than attempting to model these effects directly. Note that formation-control simulation results for fixed-wing UAVs are in [24-26, 32, 33], and experimental results are in [4, 15, 33-35].

This paper addresses formation control in a leader-fixed frame for agents with the extended unicycle dynamics. The desired interagent positions are expressed in a leader-fixed coordinate frame, which is aligned with the leader's velocity vector. Thus, the desired interagent positions vary in time as the leader-fixed frame rotates. The leader can be a physical agent or a virtual agent. The algorithms in this paper apply to formations where: the neighbor sets are such that the interagent communication structure is represented by a quasi-strongly connected graph; at least one agent has access to a measurement its position relative to the leader; and each agent has feedforward of the leader's velocity, acceleration, orientation, angular velocity, and angular acceleration. In some applications, the higher-order feedforward signals (e.g., accelerations) can be neglected. The main analytic results show that for almost all initial conditions, the agents converge to the desired relative positions with the leader and the other agents. We note that topological constraints associated with SO(m) prevent global convergence using a continuous time-invariant control [36]. The main analytic results also show that each agent's speed satisfies the hard speed constraints for all time. In addition, this paper presents an adaptive extension of the formation control algorithm to address uncertainty in the speed dynamics, which are parameterized as an unknown linear combination of known basis functions. Both the non-adaptive and adaptive formation control algorithms are demonstrated in numerical simulations. Some preliminary results related to this paper appeared in [32, 37]; however, the current paper goes significantly beyond the preliminary conference publications [32, 37] by presenting complete stability and performance analyses, and addressing uncertainty in the speed dynamics. It is also worth noting that this paper presents a significantly different control algorithm than [32, 37]. This improved algorithm effectively accommodates hard speed constraints, which were not addressed in [32].

2. Problem Formulation

Let the positive number n be the number of agents, and define the agent index set $\mathcal{I} \triangleq \{1, 2, \dots, n\}$. Define $\mathcal{P} \triangleq \{(i, j) \in \mathcal{I} \times \mathcal{I} : i \neq j\}$, which is the set of ordered pairs. Unless otherwise stated, all statements that involve the subscript i are for all $i \in \mathcal{I}$, and all statements that involve the subscripts i and j are for all $(i, j) \in \mathcal{P}$. Let $\|\cdot\|$ denote the 2-norm. The special orthogonal group SO(m) is the set of orthogonal matrices in $\mathbb{R}^{m \times m}$ with determinant one. The set of skew-symmetric matrices in $\mathbb{R}^{m \times m}$ is denoted by SO(m).

For clarity of presentation, we first develop the extended unicycle model in three-dimensional space. Thus, for the moment, let m=3. Let E be an inertial frame (e.g., the Earth frame), and let $o_{\rm E}$ be the origin of E. Let o_i be the location of the *i*th agent (e.g., the location of the *i*th vehicle's center of mass). The position of o_i relative to $o_{\rm E}$ is $\overrightarrow{q_i}$, and the *i*th agent's position $\overrightarrow{q_i}$ is resolved in E as $q_i \triangleq \overrightarrow{q_i}|_{\rm E}$. The velocity of o_i relative to $o_{\rm E}$ with respect to E is $\overrightarrow{p_i} \triangleq^{\rm E} \cdot \overrightarrow{q_i}$. Let B_i be a frame that is fixed to o_i such that $\overrightarrow{p_i}$ resolved in B_i is given by $\overrightarrow{p_i}|_{B_i} = s_i v_i$, where $v_i \in \mathbb{R}^m$ is a unit vector, and for all $t \geq 0$, $s_i(t) \in \mathbb{R}$ is the speed of the *i*th agent, which is subject to the constraint that for all $t \geq 0$, $s_i(t) \in \mathcal{S}_i \triangleq (\underline{s_i}, \overline{s_i})$, where $0 < \underline{s_i} < \overline{s_i}$. Let $R_i : [0, \infty) \to SO(m)$ be the rotation matrix from B_i to E. Thus, the *i*th agent's velocity $\overrightarrow{p_i}$ resolved in E is $\overrightarrow{p_i}|_{\rm E} = s_i R_i v_i$, which implies that

$$\dot{q}_i(t) = s_i(t)R_i(t)v_i,\tag{1}$$

where $t \geq 0$; $q_i(t) \in \mathbb{R}^m$, $s_i(t) \in \mathcal{S}_i$, and $R_i^{\mathrm{T}}(t) \in \mathrm{SO}(m)$ are the position, speed, and orientation of the *i*th agent; and $q_i(0) \in \mathbb{R}^m$ is the initial condition. Note that $R_i v_i$ is the unit vector in the direction of the velocity

 \dot{q}_i . The speed and orientation of the *i*th agent satisfy

$$\dot{s}_i(t) = f_i(s_i(t), R_i(t)) + g_i(s_i(t), R_i(t))u_i(t), \tag{2}$$

$$\dot{R}_i(t) = R_i(t)\Omega_i(t),\tag{3}$$

where $t \geq 0$; $u_i : [0, \infty) \to \mathbb{R}$ and $\Omega_i : [0, \infty) \to \text{so}(m)$ are the control inputs; $s_i(0) \in \mathcal{S}_i$ and $R_i(0) \in \text{SO}(m)$ are the initial conditions; and $f_i : \mathcal{S}_i \times \text{SO}(m) \to \mathbb{R}$ and $g_i : \mathcal{S}_i \times \text{SO}(m) \to \mathbb{R} \setminus \{0\}$ are continuous. Note that Ω_i is the skew-symmetric form of the angular velocity of B_i relative to E resolved in B_i . The agent model (1)–(3) is an extended unicycle model that includes both speed dynamics (2) and orientation kinematics (3) on SO(m), and has a hard constraint on speed s_i .

Let $o_{\rm g}$ be the location of the leader, which can be a physical agent (e.g., a vehicle) or a virtual agent. The position of $o_{\rm g}$ relative to $o_{\rm E}$ is $\overrightarrow{q_{\rm g}}$, and the leader's position $\overrightarrow{q_{\rm g}}$ is resolved in E as $q_{\rm g} \triangleq \overrightarrow{q_{\rm g}}|_{\rm E}$, which is assumed to be twice continuously differentiable. The velocity of $o_{\rm g}$ relative to $o_{\rm E}$ with respect to E is $\overrightarrow{p_{\rm g}} \triangleq^{\rm E} \overrightarrow{q_{\rm g}}$. Let B_g be a frame that is fixed to $o_{\rm g}$ and has orthogonal unit vectors $\hat{\imath}_{\rm g}$, $\hat{\jmath}_{\rm g}$, and $\hat{k}_{\rm g}$, where $\hat{\imath}_{\rm g}$ is parallel to the leader's velocity vector $\overrightarrow{p_{\rm g}}$, and the rotation matrix from $B_{\rm g}$ to E is $R_{\rm g}:[0,\infty)\to {\rm SO}(m)$, which is assumed to be twice continuously differentiable.

This paper addresses the problem of formation control in the leader-fixed frame B_g . Let $\delta_i \in \mathbb{R}^m$ be the desired position of o_i relative to o_g resolved in B_g . Thus, for all $(i,j) \in \mathcal{P}$, $\delta_{ij} \triangleq \delta_i - \delta_j$ is the desired position of o_i relative to o_j resolved in B_g . Our objective is to design controls u_i and Ω_i such that:

- (O1) For all $(i,j) \in \mathcal{P}$, $\lim_{t\to\infty} R_{\mathbf{g}}^{\mathrm{T}}(t)[q_i(t) q_j(t)] = \delta_{ij}$.
- (O2) For all $i \in \mathcal{I}$, $\lim_{t \to \infty} [\dot{q}_i(t) \dot{q}_g(t) \dot{R}_g(t)\delta_i] = 0$.
- (O3) For all $i \in \mathcal{I}$, $\lim_{t \to \infty} R_g^{\mathrm{T}}(t)[q_i(t) q_g(t)] = \delta_i$.
- (O4) For all $i \in \mathcal{I}$ and for all $t \geq 0$, $s_i(t) \in \mathcal{S}_i$.

Objective (O1) states that the interagent positions approach the desired values. Objective (O2) states that each agent's velocity with respect to B_g approaches the leader's velocity with respect to B_g , and (O3) states that each agent approaches its desired relative position with the leader. Objective (O4) states that the agents' speed constraints are satisfied. If (O3) is satisfied, then (O1) is satisfied. However, we enumerate these objectives independently because some results in this paper show that if no agents have access to a measurement of the leader's position, then (O1) is satisfied but (O3) is not.

Notably, it is not possible to satisfy the formation objectives (O1)–(O3) and the speed constraint (O4) for an arbitrary leader trajectory (i.e., q_g and R_g). More specifically, if (O2) is satisfied, then the *i*th agent's velocity \dot{q}_i converges to $\dot{q}_g + \dot{R}_g \delta_i$. Thus, (O2) implies that we want the *i*th agent's speed $\|\dot{q}_i(t)\|$ to equal $\|\dot{q}_g(t) + \dot{R}_g(t)\delta_i\|$. However, (O4) requires that the *i*th agent's speed satisfies $\|\dot{q}_i(t)\| \in \mathcal{S}_i$. Thus, if the *i*th agent's speed equals $\|\dot{q}_g(t) + \dot{R}_g(t)\delta_i\|$ and satisfies $\|\dot{q}_i(t)\| \in \mathcal{S}_i$, then the leader trajectory must satisfy $\|\dot{q}_g(t) + \dot{R}_g(t)\delta_i\| \in \mathcal{S}_i$. Therefore, we make the following assumption:

(A1) For all
$$i \in \mathcal{I}$$
, there exists $\kappa_i > 0$ such that for all $t \geq 0$, $\|\dot{q}_{\mathrm{g}}(t) + \dot{R}_{\mathrm{g}}(t)\delta_i\| \in (\underline{s}_i + \kappa_i, \bar{s}_i - \kappa_i)$.

Assumption (A1) implies that for all $t \geq 0$, $\|\dot{q}_{\rm g}(t) + \dot{R}_{\rm g}(t)\delta_i\|$ is contained in a proper subset of \mathcal{S}_i . However, $\kappa_i > 0$ can be arbitrarily close to zero. Furthermore, as κ_i approaches zero, (A1) approaches the condition $\|\dot{q}_{\rm g}(t) + \dot{R}_{\rm g}(t)\delta_i\| \in \mathcal{S}_i$, which is necessary to simultaneously satisfy $\dot{q}_i(t)$ equals $\dot{q}_{\rm g}(t) + \dot{R}_{\rm g}(t)\delta_i$ and $\|\dot{q}_i(t)\| \in \mathcal{S}_i$. In many practical applications (e.g., fixed-wing UAV formations or ground robot formations), the leader is a physical or virtual agent, whose motion can be constrained to ensure that (A1) is satisfied.

Although the physical (i.e., frame-based) formulation of the control problem is described in three dimensions, the methods in this paper apply to all $m \in \{2, 3, 4, \ldots\}$. Thus, for generality, the remainder of this paper considers the extended unicycle model (1)–(3) and control objectives (O1)–(O4), where $m \in \{2, 3, 4, \ldots\}$. The extended unicycle model and formation control problem described above have physical applications for m=2 and m=3. For example, m=2 is for planar motion, which can apply to a variety of ground-robotic applications. Similarly, the extended unicycle dynamics for three-dimensional motion (i.e., m=3) is applicable to fixed-wing UAVs.

The interagent communication (i.e., feedback) structure is represented using a directed graph. The agent index set \mathcal{I} is the vertex set of the directed graph, and the n elements of \mathcal{I} are the vertices. Let $\mathcal{E} \subset \mathcal{I} \times \mathcal{I}$ be the directed edge set. The elements of \mathcal{E} are the directed edges. Then, the directed graph is $\mathcal{G} = (\mathcal{I}, \mathcal{E})$. The directed graph $\mathcal{G} = (\mathcal{I}, \mathcal{E})$ has a walk of length l from $v_0 \in \mathcal{I}$ to $v_l \in \mathcal{I}$ if there exists an (l+1)-tuple $(v_0, v_1, \ldots, v_l) \in \mathcal{I} \times \mathcal{I} \times \cdots \times \mathcal{I}$ such that for all $j \in \{1, 2, \ldots, l\}, (v_{j-1}, v_j) \in \mathcal{E}$. The directed graph $\mathcal{G} = (\mathcal{I}, \mathcal{E})$ is quasi-strongly connected if there exists $\ell \in \mathcal{I}$ such that for all $j \in \mathcal{I} \setminus \{\ell\}, \mathcal{G} = (\mathcal{I}, \mathcal{E})$ has a walk from ℓ to j. In this case, ℓ is a center vertex of the quasi-strongly connected directed graph $\mathcal{G} = (\mathcal{V}, \mathcal{E})$.

Define the neighbor set $\mathcal{N}_i \triangleq \{j \in \mathcal{I} : (j,i) \in \mathcal{E}\}$. Without loss of generality, we assume that for all $i \in \mathcal{I}$, $(i,i) \notin \mathcal{E}$, which implies that $i \notin \mathcal{N}_i$. In this paper, we assume that $\mathcal{G} = (\mathcal{I}, \mathcal{E})$ is quasi-strongly connected, and that the *i*th agent has access to measurements of $\{q_j - q_i\}_{j \in \mathcal{N}_i}$ and $\{\dot{q}_j - \dot{q}_i\}_{j \in \mathcal{N}_i}$ for feedback. We also assume that $\mathcal{G} = (\mathcal{I}, \mathcal{E})$ has a center vertex ℓ such that the ℓ th agent has a measurement of its position relative to the leader $q_g - q_i$. Thus, the algorithm presented in this paper only requires that one agent has a measurement of $q_g - q_i$. Finally, we assume that each agent has access to measurements of \dot{q}_g , \ddot{q}_g , \dot{R}_g , and \ddot{R}_g for feedfoward. In many practical applications such as fixed-wing UAV formation flying, it is reasonable to assume that each agent (e.g., UAV) has access to the required feedforward information regarding the leader through communication or direct measurement, or because the leader's maneuvers are specified a priori. In addition, from a practical implementation perspective, leader maneuvers often have relatively small translational acceleration \ddot{q}_g and rotational acceleration \ddot{R}_g . In this case, the algorithm in this paper can be effectively implemented with $\ddot{q}_g = 0$ and $\ddot{R}_g = 0$.

3. Formation Control Algorithm

This section presents a formation control algorithm that achieves (O1)–(O4) for agents modeled by the extended unicycle dynamics (1)–(3), where the speed dynamics (2) are known, that is, the functions f_i and g_i are known. In Section 5, we present and analyze an adaptive extension of the algorithm, which addresses uncertainty in the speed dynamics (2).

Let $\nu_1, \nu_2 > 0$, and consider $\sigma : [0, \infty) \to (0, \frac{1}{\sqrt{\nu_1}}]$ defined by

$$\sigma(a) \triangleq 1/\sqrt{\nu_1 + \nu_2 a}.\tag{4}$$

Furthermore, consider $\rho: \mathbb{R}^m \to \mathbb{R}^m$ defined by

$$\rho(x) \triangleq \sigma(\|x\|^2)x,\tag{5}$$

and note that $\sup_{x \in \mathbb{R}^m} \|\rho(x)\| = 1/\sqrt{\nu_2}$. Also, consider $\rho' : \mathbb{R}^m \to \mathbb{R}^{m \times m}$ defined by

$$\rho'(x) \triangleq \frac{\partial \rho(x)}{\partial x} = \sigma(\|x\|^2) I_m - \nu_2 \sigma^3(\|x\|^2) x x^{\mathrm{T}}, \tag{6}$$

where I_m is the $m \times m$ identity matrix.

Define the feedback function

$$\phi_i \triangleq \alpha_i (q_g - q_i + R_g \delta_i) + \sum_{j \in \mathcal{N}_i} \beta_{ij} (q_j - q_i + R_g \delta_{ij}), \tag{7}$$

where $\alpha_i \geq 0$; for all $j \in \mathcal{N}_i$, $\beta_{ij} > 0$; and for all $j \notin \mathcal{N}_i$, $\beta_{ij} = 0$. The *i*th agent can compute the feedback function ϕ_i using $\{q_j - q_i\}_{j \in \mathcal{N}_i}$, and $q_g - q_i$ if $\alpha_i > 0$. The approach in this paper only requires that one agent has a measurement of $q_g - q_i$. Specifically, we assume that there exists a center vertex ℓ of $\mathcal{G} = (\mathcal{I}, \mathcal{E})$ such that $\alpha_{\ell} > 0$.

Let $k_i \in (0, \kappa_i \sqrt{\nu_2})$, and define the *i*th agent's desired velocity

$$p_{\mathrm{d},i} \triangleq \dot{q}_{\mathrm{g}} + \dot{R}_{\mathrm{g}} \delta_{i} + k_{i} \rho(\phi_{i}),$$
 (8)

and define the ith agent's desired speed

$$s_{\mathrm{d},i} \triangleq \|p_{\mathrm{d},i}\|. \tag{9}$$

Note that (A1), (4), (5), (8), and (9) imply that $p_{d,i}$ and $s_{d,i}$ are bounded. In fact, the next result shows that for all $t \geq 0$, $s_{d,i}(t)$ is contained in $S_{d,i} \triangleq (\underline{s}_i + \varepsilon_d, \overline{s}_i - \varepsilon_d)$, where

$$\varepsilon_{\rm d} \triangleq \min_{i \in \mathcal{I}} \left(\kappa_i - \frac{k_i}{\sqrt{\nu_2}} \right),$$

which is positive because $k_i \in (0, \kappa_i \sqrt{\nu_2})$. This result follows immediately from substituting (8) into (9), using the triangle inequality, and using (A1).

Proposition 1. Assume that (A1) is satisfied. Then, for all $t \geq 0$, $s_{d,i}(t) \in \mathcal{S}_{d,i} \subset \mathcal{S}_i$.

Next, define the time derivatives of $p_{d,i}$ and $s_{d,i}$, which are

$$\dot{p}_{d,i} \triangleq \ddot{q}_g + \ddot{R}_g \delta_i - k_i \rho'(\phi_i) \left[\alpha_i (\dot{q}_i - \dot{q}_g - \dot{R}_g \delta_i) + \sum_{j \in \mathcal{N}_i} \beta_{ij} (\dot{q}_i - \dot{q}_j - \dot{R}_g \delta_{ij}) \right], \tag{10}$$

$$\dot{s}_{\mathrm{d},i} \triangleq \frac{\partial s_{\mathrm{d},i}}{\partial p_{\mathrm{d},i}} \dot{p}_{\mathrm{d},i} = \frac{1}{s_{\mathrm{d},i}} p_{\mathrm{d},i}^{\mathrm{T}} \dot{p}_{\mathrm{d},i}. \tag{11}$$

To enforce the speed constraint (O4), we consider the asymmetric speed barrier function $h_i : \mathcal{S}_i \times \mathcal{S}_{d,i} \to (0,\infty)$ defined by

$$h_i(s_i, s_{d,i}) \triangleq \frac{(\bar{s}_i - s_{d,i})(s_{d,i} - \underline{s}_i)}{(\bar{s}_i - s_i)(s_i - \underline{s}_i)},\tag{12}$$

which is inspired by the asymmetric barrier functions in [38]. Note that for all $(s_i, s_{d,i}) \in \mathcal{S}_i \times \mathcal{S}_{d,i}$, $h_i(s_i, s_{d,i}) > \underline{h}_i \triangleq 4\varepsilon_d(\bar{s}_i - \underline{s}_i - \varepsilon_d)/(\bar{s}_i - \underline{s}_i)^2$, which is positive. Furthermore, $h_i(s_i, s_{d,i})$ diverges to infinity as s_i approaches its upper bound \bar{s}_i or lower bound \underline{s}_i . In addition, define the partial derivatives

$$\frac{\partial h_i(s_i, s_{d,i})}{\partial s_i} \triangleq -\frac{(\bar{s}_i + \underline{s}_i - 2s_i)}{(\bar{s}_i - s_i)(s_i - s_i)} h_i(s_i, s_{d,i}),\tag{13}$$

$$\frac{\partial h_i(s_i, s_{d,i})}{\partial s_{d,i}} \triangleq \frac{(\bar{s}_i + \underline{s}_i - 2s_{d,i})}{(\bar{s}_i - s_i)(s_i - \underline{s}_i)}.$$
(14)

Next, let $\gamma_i, \eta_i > 0$, and consider the formation control

$$u_{i} = \frac{-1}{g_{i}(s_{i}, R_{i})} \left(f_{i}(s_{i}, R_{i}) + \frac{\gamma_{i}(s_{i} - s_{d,i})h_{i}(s_{i}, s_{d,i})}{\mu_{i}(s_{i}, s_{d,i})} + \dot{s}_{d,i} \left(\frac{(s_{i} - s_{d,i})}{\mu_{i}(s_{i}, s_{d,i})} \frac{\partial h_{i}(s_{i}, s_{d,i})}{\partial s_{d,i}} - \frac{h_{i}(s_{i}, s_{d,i})}{\mu_{i}(s_{i}, s_{d,i})} \right) \right), \quad (15)$$

$$\Omega_{i} = \eta_{i} s_{d,i} \left(R_{i}^{T} p_{d,i} v_{i}^{T} - v_{i} p_{d,i}^{T} R_{i} \right) + \frac{1}{s_{d,i}^{2}} R_{i}^{T} \left(\dot{p}_{d,i} p_{d,i}^{T} - p_{d,i} \dot{p}_{d,i}^{T} \right) R_{i}, \tag{16}$$

where $\mu_i: \mathcal{S}_i \times \mathcal{S}_{d,i} \to \mathbb{R}$ is defined by

$$\mu_i(s_i, s_{d,i}) \triangleq h_i(s_i, s_{d,i}) + (s_i - s_{d,i}) \frac{\partial h_i(s_i, s_{d,i})}{\partial s_i}.$$
 (17)

Since for all $t \geq 0$, $s_{d,i}(t) \in \mathcal{S}_{d,i}$, it follows that Ω_i , which involves division by $s_{d,i}^2$, is well defined. In the next section, we show that for all $t \geq 0$, $s_i(t) \in \mathcal{S}_i$. In this case, the next result demonstrates that for all $t \geq 0$, $\mu_i(s_i(t), s_{d,i}(t)) > 0$, which implies that u_i , which involves division by $\mu_i(s_i, s_{d,i})$, is well defined.

Proposition 2. For all
$$(s_i, s_{d,i}) \in \mathcal{S}_i \times \mathcal{S}_{d,i}, \mu_i(s_i, s_{d,i}) > 0.$$

The proof of Proposition 2 is omitted for space considerations; however, the proof follows from direct computation. Specifically, it can be shown that the numerator of $\mu_i(s_i, s_{\mathrm{d},i})$ has only positive local minima on $\mathcal{S}_i \times \mathcal{S}_{\mathrm{d},i}$. Since, in addition, this numerator is continuous on $\mathcal{S}_i \times \mathcal{S}_{\mathrm{d},i}$, it follows that it is positive on $\mathcal{S}_i \times \mathcal{S}_{\mathrm{d},i}$. Similarly, it can be shown that the denominator of $\mu_i(s_i, s_{\mathrm{d},i})$ is positive on $\mathcal{S}_i \times \mathcal{S}_{\mathrm{d},i}$. Thus, $\mu_i(s_i, s_{\mathrm{d},i})$ is positive on $\mathcal{S}_i \times \mathcal{S}_{\mathrm{d},i}$, which confirms the result.

The control (4)–(17) involves the parameters $\nu_1 > 0$, $\nu_2 > 0$, $\alpha_i \ge 0$, $\beta_{ij} \ge 0$, $k_i \in (0, \kappa_i \sqrt{\nu_2})$, $\gamma_i > 0$, and $\eta_i > 0$. Increasing the speed gain γ_i tends to cause the speed s_i to converge more quickly to the desired speed $s_{d,i}$. Similarly, increasing the attitude gain η_i tends to cause the pointing direction $R_i v_i$ to converge more quickly to the desired pointing direction $p_{d,i}/s_{d,i}$. However, increasing γ_i and η_i also tends to increase the magnitude of the controls u_i and Ω_i . Selecting k_i close to the upper limit $\kappa_i \sqrt{\nu_2}$ tends to make the desired velocity (8) more responsive to the formation term $\rho(\phi_i)$, which, in turn, tends to make the agents converge more quickly to the desired interagent positions because ϕ_i contains the formation terms $\beta_{ij}(q_j - q_i + R_g \delta_{ij})$. The upper limit $\kappa_i \sqrt{\nu_2}$ on k_i is imposed to guarantee that the desired speed $s_{d,i}$ is in the admissible range $S_{d,i}$. This upper limit decreases as ν_2 decreases. The parameters ν_1 and ν_2 also affect the shape of the nonlinear functions σ and ρ . If $\nu_1/\nu_2 \gg 1$, then for all ϕ_i such that $\|\phi_i\| \ll \nu_1/\nu_2$, it follows that $\rho(\phi_i) \approx \frac{1}{\sqrt{\nu_i}} \phi_i$. In this case, the desired velocity (8) is approximately linear in the feedback function ϕ_i , which itself is linear in the formation terms that appear in (7). In contrast, if $\nu_1/\nu_2 \ll 1$, then for all ϕ_i such that $\|\phi_i\| \gg \nu_1/\nu_2$, it follows that $\rho(\phi_i) \approx \frac{1}{\|\phi_i\|\sqrt{\nu_2}}\phi_i$, which implies that $\rho(\phi_i)$ changes directions but $\|\rho(\phi_i)\|$ is approximately constant. In this case, its worth noting that σ , which is used in ρ , approximates a switch because it transitions rapidly from its maximum value $1/\sqrt{\nu_1}$ to its minimum value 0 as its argument increases from 0. The formation gains α_i and β_{ij} determine how sensitive ϕ_i is to error in the *i*th agent's position relative to the leader and to error in the ith agent's position relative to the jth agent, respectively. Selecting α_i and β_{ij} small tends to decrease $\|\phi_i\|$, which tends to cause $\rho(\phi_i)$ to operate in the approximately linear range described above. In contrast, selecting α_i and β_{ij} large tends to increase $\|\phi_i\|$, which tends to cause $\rho(\phi_i)$ to operate in the range where $\rho(\phi_i)$ has constant norm but changing direction.

4. Stability Analysis

In this section, we analyze the closed-loop dynamics (1)–(17). Define the position error

$$\zeta_i \triangleq q_i - q_g - R_g \delta_i, \tag{18}$$

and substituting (18) into (7) yields

$$\phi_i = -\alpha_i \zeta_i - \sum_{j \in \mathcal{N}_i} \beta_{ij} (\zeta_i - \zeta_j). \tag{19}$$

For all $t \geq 0$, define

$$\zeta(t) \triangleq \begin{bmatrix} \zeta_1(t) \\ \vdots \\ \zeta_n(t) \end{bmatrix} \in \mathbb{R}^{mn}, \qquad \phi(t) \triangleq \begin{bmatrix} \phi_1(t) \\ \vdots \\ \phi_n(t) \end{bmatrix} \in \mathbb{R}^{mn}.$$

Let $L \in \mathbb{R}^{n \times n}$ be such that the (i, j)th element is $L_{(i, j)} = -\beta_{ij}$, and the (i, i)th element is $L_{(i, i)} = \sum_{j \in \mathcal{N}_i} \beta_{ij}$. Note that L is the Laplacian of the directed graph $\mathcal{G} = (\mathcal{I}, \mathcal{E})$, where for all $(i, j) \in \mathcal{E}$, we associate the weight β_{ij} . Furthermore, define

$$A \triangleq \operatorname{diag}\left(\alpha_1, \dots, \alpha_n\right) \in \mathbb{R}^{n \times n},$$

where $diag(\cdot)$ denotes the diagonal matrix whose diagonal elements are given by the arguments of the operator. Then, it follows from (19) that

$$\phi = -[(L+A) \otimes I_m]\zeta,\tag{20}$$

where \otimes is the Kronecker product. Note that (20) can be viewed as a change of variables between the position error ζ and ϕ . This change of variables is related to the one used in [19]. The following result provides sufficient conditions such that L + A is nonsingular, which implies that (20) is a bijection. This result follows from [39, Lemma 1].

Lemma 1. Assume that $\mathcal{G} = (\mathcal{I}, \mathcal{E})$ is quasi-strongly connected, and assume that there exists a center vertex ℓ of $\mathcal{G} = (\mathcal{I}, \mathcal{E})$ such that $\alpha_{\ell} > 0$. Then, L + A is nonsingular.

Remark 1. Lemma 1 provides sufficient conditions such that L+A is nonsingular; however, theses conditions are not necessary. For example, if for all $i \in \mathcal{I}$, $\alpha_i > 0$, then L+A is nonsingular. This situation arises if each agent has a measurement of its position relative to the leader. As another example, if $\mathcal{G} = (\mathcal{I}, \mathcal{E})$ is the union of l quasi-strongly connected graphs and each of those graphs has a center vertex ℓ_1, \ldots, ℓ_l such that $\alpha_{\ell_1}, \ldots, \alpha_{\ell_l} > 0$, then L+A is nonsingular [39, Lemma 1]. The stability results in this paper rely on the assumption that L+A is nonsingular, and Lemma 1 provides one communication (i.e., feedback) structure under which L+A is nonsingular. However, as discussed above, there are other communication structures that yield nonsingular L+A, and the results in this paper also apply to those communication structures.

Next, differentiating (18), and using (1), (5), and (8) implies that

$$\dot{\zeta}_i = s_i R_i v_i - \dot{q}_g - \dot{R}_g \delta_i
= k_i \rho(\phi_i) + s_i R_i v_i - p_{d,i}
= k_i \sigma(\|\phi_i\|^2) \phi_i + s_i R_i v_i - p_{d,i}.$$
(21)

Consider $B: \mathbb{R}^{mn} \to \mathbb{R}^{mn \times mn}$ defined by

$$B(\phi) \triangleq \left(\operatorname{diag}\left(k_1 \sigma(\|\phi_1\|^2), \dots, k_n \sigma(\|\phi_n\|^2)\right)\right) \otimes I_m, \tag{22}$$

and it follows from (21) that

$$\dot{\zeta} = B(\phi)\phi + \sum_{i \in \mathcal{I}} (d_i \otimes I_m)(s_i R_i v_i - p_{d,i}), \tag{23}$$

where

$$d_i \triangleq \begin{bmatrix} 0_{1 \times i-1} & 1 & 0_{1 \times n-i} \end{bmatrix}^{\mathrm{T}} \in \mathbb{R}^n.$$

Differentiating (20) yields

$$\dot{\phi} = -\left[(L+A) \otimes I_m \right] \dot{\zeta},\tag{24}$$

and using (23) implies that

$$\dot{\phi} = -\left[(L+A) \otimes I_m \right] B(\phi)\phi - \sum_{i \in \mathcal{I}} \left[(L+A)d_i \otimes I_m \right] \left(s_i R_i v_i - p_{d,i} \right). \tag{25}$$

The following result is used to analyze stability. This result follows from [23, Theorem 4.25].

Lemma 2. Assume that L + A is nonsingular. Then, there exists a positive-definite diagonal matrix $D \in \mathbb{R}^{n \times n}$ such that $(L + A)^{\mathrm{T}}D + D(L + A)$ is positive definite.

The remainder of the stability analysis is divided into four subsections. The first three subsections examine the closed-loop position dynamics, speed dynamics, and orientation kinematics, respectively. Each subsection presents a Lyapunov-like function, which is used to analyze the associated component of the closed-loop behavior. Then, the final subsection combines these Lyapunov-like functions to analyze the full closed-loop dynamics (1)–(17).

First, Section 4.1 considers the position dynamics (1) under the assumption that each agent's velocity $s_i R_i v_i$ is a control variable, which is equivalent to the simplified scenario with single-integrator agent dynamics. In this case, if the velocity control is equal to the desired velocity (i.e., $s_i R_i v_i = p_{d,i}$), then (O1)–(O4) are satisfied. The preliminary result in Section 4.1 is not directly applicable to the extended unicycle model (1)–(3) because it neglects the speed dynamics (2) and orientation kinematics (3). Nevertheless, this preliminary result is informative because it shows that if the velocity $s_i R_i v_i$ is equal to the desired velocity $p_{d,i}$, then the control objectives are achieved. Moreover, the Lyapunov-like function from this simplified analysis is used in the full analysis.

Next, Section 4.2 examines the speed dynamics (2) and the associated control (15). This subsection demonstrates that the speed constraint (O4) is satisfied, and that the speed s_i converges to the desired speed $s_{d,i}$. Then, Section 4.3 examines the orientation kinematics (3) and the associated control (16). This subsection shows the point direction $R_i v_i$ converges to the desired pointing direction $p_{d,i}/s_{d,i}$. Together,

Sections 4.2 and 4.3 show that the velocity $s_i R_i v_i$ converges to the desired velocity $p_{d,i}$, which, combined with the preliminary result in Section 4.1 (which assumes that $s_i R_i v_i = p_{d,i}$), provides the intuition for the full closed-loop analysis.

Finally, Section 4.4 analyzes the full closed-loop dynamics (1)–(17). This analysis combines the three Lyapunov-like functions used in each of Sections 4.1–4.3 to show that objectives (O1)–(O4) are satisfied.

4.1. Position Dynamics with Direct Velocity Control

This section analyzes the closed-loop position dynamics (25) under the assumption that each agent's velocity $s_i R_i v_i$ is a control variable, specifically, $s_i R_i v_i = p_{d,i}$. In this case, (1) can be viewed as a single integrator with feedback control $s_i R_i v_i = p_{d,i}$.

Let $D \in \mathbb{R}^{n \times n}$ be the positive-definite diagonal matrix given by Lemma 2, and consider the Lyapunov-like function $V_0 : \mathbb{R}^m \times \cdots \times \mathbb{R}^m \to [0, \infty)$ defined by

$$V_0(\phi_1, \dots, \phi_n) \triangleq \sum_{i \in \mathcal{I}} k_i d_i^{\mathrm{T}} D d_i \int_0^{\|\phi_i\|^2} \sigma(s) \, \mathrm{d}s = \frac{2}{\nu_2} \sum_{i \in \mathcal{I}} k_i d_i^{\mathrm{T}} D d_i \left(\sqrt{\nu_1 + \nu_2 \|\phi_i\|^2} - \sqrt{\nu_1} \right). \tag{26}$$

Next, define the Lyapunov-like derivative

$$\dot{V}_0(\phi_1, \dots, \phi_n) \triangleq \sum_{i \in \mathcal{I}} \frac{\partial V_0(\phi_1, \dots, \phi_n)}{\partial \phi_i} \dot{\phi}_i.$$
 (27)

The following preliminary result considers the case where the velocity $s_i R_i v_i$ is a control variable, specifically, $s_i R_i v_i = p_{d,i}$.

Proposition 3. Consider the closed-loop dynamics (25), which consists of (1) and (4)–(8), and assume that $s_i R_i v_i = p_{d,i}$. Assume that L + A is nonsingular. Then, the following statements hold:

i) For all $(\phi_1, \dots, \phi_n) \in \mathbb{R}^m \times \dots \times \mathbb{R}^m$,

$$\dot{V}_0(\phi_1,\ldots,\phi_n) = -\phi^{\mathrm{T}}B(\phi)\Big[\Big((L+A)^{\mathrm{T}}D + D(L+A)\Big) \otimes I_m\Big]B(\phi)\phi,$$

which is negative definite.

- ii) $\phi(t) \equiv 0$ is a globally asymptotically stable equilibrium of (25) with $s_i R_i v_i = p_{d,i}$.
- iii) For all $q_i(0) \in \mathbb{R}^m$, (O1)–(O3) are satisfied.
- iv) If (A1) is satisfied, then for all $q_i(0) \in \mathbb{R}^m$, (O4) is satisfied.

Proof. Since $s_i R_i v_i = p_{d,i}$, it follows from (25) that

$$\dot{\phi} = -\left[(L+A) \otimes I_m \right] B(\phi) \phi. \tag{28}$$

Since D is diagonal, it follows from (26), (27), and (22) that

$$\dot{V}_0(\phi_1, \dots, \phi_n) = 2 \sum_{i \in \mathcal{I}} k_i d_i^{\mathrm{T}} D d_i \sigma(\|\phi_i\|^2) \phi_i^{\mathrm{T}} \dot{\phi}_i = 2\phi^{\mathrm{T}} B(\phi) \Big(D \otimes I_m \Big) \dot{\phi}. \tag{29}$$

Evaluating (29) along the trajectories of (28) yields

$$\dot{V}_0(\phi_1, \dots, \phi_n) = -2\phi^{\mathrm{T}} B(\phi) \Big(D(L+A) \otimes I_m \Big) B(\phi) \phi
= -\phi^{\mathrm{T}} B(\phi) \Big[\Big((L+A)^{\mathrm{T}} D + D(L+A) \Big) \otimes I_m \Big] B(\phi) \phi.$$
(30)

Since L + A is nonsingular, Lemma 2 implies that $P \triangleq (L + A)^{T}D + D(L + A)$ is positive definite. Thus, the minimum eigenvalue of P, which is denoted by $\lambda_{\min}(P)$, is positive, and it follows from (22) and (30) that

$$\dot{V}_0(\phi_1, \dots, \phi_n) \le -\lambda_{\min}(P)\phi^{\mathrm{T}}B^2(\phi)\phi = -\lambda_{\min}(P)\sum_{i \in \mathcal{I}} k_i^2 \sigma^2(\|\phi_i\|^2)\phi_i^{\mathrm{T}}\phi_i.$$
(31)

Since $\lambda_{\min}(P) > 0$ and $k_i > 0$, it follows from (4) and (31) that \dot{V}_0 is negative definite, which confirms i). Since V_0 is positive definite and radially unbounded, and \dot{V}_0 is negative definite, it follows that the origin is a globally asymptotically stable equilibrium of (25), which confirms ii).

To show iii), it follows from (20) that $\zeta = -[(L+A)^{-1} \otimes I_m]\phi$. Since, in addition, $\lim_{t\to\infty}\phi(t) = 0$, it follows that $\lim_{t\to\infty}\zeta(t) = 0$. Since $R_{\rm g}(t)$ is bounded and $\lim_{t\to\infty}\zeta_i(t) = 0$, it follows from (18) that $\lim_{t\to\infty}R_{\rm g}^{\rm T}(t)[q_i(t)-q_j(t)]=\lim_{t\to\infty}R_{\rm g}^{\rm T}(t)[\zeta_i(t)-\zeta_j(t)+R_{\rm g}(t)\delta_{ij}]=\delta_{ij}$ and $\lim_{t\to\infty}R_{\rm g}^{\rm T}(t)q_i(t)=\lim_{t\to\infty}R_{\rm g}^{\rm T}(t)[\zeta_i(t)+R_{\rm g}(t)\delta_i]=\delta_i$, which confirms (O1) and (O3). Since $s_iR_iv_i=p_{{\rm d},i}$ and $\lim_{t\to\infty}\phi_i(t)=0$, it follows from (4) and (21) that $\lim_{t\to\infty}\dot{\zeta}_i(t)=0$, which confirms (O2), thus verifying iii).

To show iv), assume that (A1) is satisfied. Thus, Proposition 1 implies that for all $t \geq 0$, $s_{d,i}(t) \in \mathcal{S}_{d,i}$. Since, in addition, $s_i = s_{d,i}$ and $\mathcal{S}_{d,i} \subset \mathcal{S}_i$ it follows that for all $t \geq 0$, $s_i(t) \in \mathcal{S}_i$, which confirms iv).

Remark 2. Proposition 3 relies on the assumption that L+A is nonsingular, and Lemma 1 demonstrates that this assumption holds if $\mathcal{G}=(\mathcal{I},\mathcal{E})$ is quasi-strongly connected with a center vertex that has feedback of the leader's position (i.e., $\alpha_{\ell}>0$ for the center vertex ℓ). If no agent has feedback of the leader's position (i.e., for all $i\in\mathcal{I}, \alpha_i=0$), then L+A=L is singular. However, under the assumption that \mathcal{G} is strongly connected, it is possible to modify the proof of Proposition 3 to demonstrate that a subset of the formation objective are satisfied. Specifically, [40] shows that if \mathcal{G} is strongly connected, then there exists a positive-definite diagonal matrix $D_2 \in \mathbb{R}^{n \times n}$ such that $L^T D_2 + D_2 L$ is positive semidefinite with a simple eigenvalue at zero and the ones vector is the associated eigenvector. In this case, we can consider the Lyapunov-like function (26), where D is replaced by D_2 , and use steps similar to those in the proof of Proposition 3 to show that $\phi(t) \equiv 0$ is a globally asymptotically stable equilibrium. However, since L+A=L is singular, it follows that the change of variables (24) is not a bijection. Thus, although ϕ_i converges to zero, ζ_i does not generally converge to zero. Nevertheless, it can be demonstrated that (O1) and (O2) are satisfied even though (O3) is not. Additionally, if (A1) is satisfied, then (O4) is satisfied.

Proposition 3 shows that if $s_i R_i v_i = p_{d,i}$, then (O1)–(O3) are satisfied, and if, in addition, (A1) is satisfied, then (O4) is satisfied. However, the speed s_i and pointing direction $R_i v_i$ are not controls. Instead, s_i is determined from (2), which has control input u_i , and $R_i v_i$ is determined from (3), which has control input Ω_i . Thus, the next two subsections examine the closed-loop speed dynamics and orientation kinematics. Then, we analyze the full closed-loop dynamics (1)–(17). Note that the preliminary result Proposition 3 is not used in any of the subsequent analysis, but the Lyapunov-like function (26) plays a critical role in analyzing the full closed-loop dynamics.

4.2. Speed Dynamics

In this section, we examine the speed dynamics (2) and the associated control (15) to show that the speed constraint (O4) is satisfied. Define the speed error

$$\tilde{s}_i \triangleq s_i - s_{\mathrm{d},i}$$
.

Differentiating \tilde{s}_i and using (2) and (15) implies that

$$\dot{\tilde{s}}_i = \frac{-\tilde{s}_i}{\mu_i(s_i, s_{d,i})} \left[\gamma_i h_i(s_i, s_{d,i}) + \left(\frac{\partial h_i(s_i, s_{d,i})}{\partial s_{d,i}} + \frac{\partial h_i(s_i, s_{d,i})}{\partial s_i} \right) \dot{s}_{d,i} \right]. \tag{32}$$

Consider the Lyapunov-like function $Z_i : \mathbb{R} \times \mathcal{S}_{d,i} \to [0,\infty)$ defined by

$$Z_i(\tilde{s}_i, s_{d,i}) \triangleq \frac{1}{2} h_i^2(s_i, s_{d,i}) \tilde{s}_i^2, \tag{33}$$

and define the Lyapunov-like derivative

$$\dot{Z}_{i}(\tilde{s}_{i}, s_{d,i}) \triangleq \frac{\partial Z_{i}(\tilde{s}_{i}, s_{d,i})}{\partial \tilde{s}_{i}} \dot{\tilde{s}}_{i} + \frac{\partial Z_{i}(\tilde{s}_{i}, s_{d,i})}{\partial s_{d,i}} \dot{s}_{d,i}.$$
(34)

The next result shows that if (A1) is satisfied and $s_i(0) \in \mathcal{S}_i$, then for all $t \geq 0$, $s_i(t) \in \mathcal{S}_i$ and $\lim_{t\to\infty} \tilde{s}_i(t) = 0$.

Proposition 4. Consider the closed-loop dynamics (32), which consists of (2), (4)–(15), and (17). Assume that (A1) is satisfied. Then, the following statements hold:

- i) For all $(s_i, s_{d,i}) \in \mathcal{S}_i \times \mathcal{S}_{d,i}$, $\dot{Z}_i(\tilde{s}_i, s_{d,i}) = -\gamma_i h_i^2(s_i, s_{d,i}) \tilde{s}_i^2 \leq -\gamma_i \underline{h}_i^2 \tilde{s}_i^2$, where $\underline{h}_i \triangleq \frac{4(\bar{s}_i \underline{s}_i \varepsilon_d)\varepsilon_d}{(\bar{s}_i s_i)^2} > 0$.
- ii) For all $s_i(0) \in \mathcal{S}_i$, (O4) is satisfied.
- iii) For all $s_i(0) \in \mathcal{S}_i$, $\lim_{t \to \infty} \tilde{s}_i(t) = 0$.

Proof. Evaluating (34) along the trajectories of (32) yields

$$\dot{Z}_{i}(\tilde{s}_{i}, s_{\mathrm{d},i}) = h_{i}(s_{i}, s_{\mathrm{d},i})\tilde{s}_{i} \left[\left(\frac{\partial h_{i}(s_{i}, s_{\mathrm{d},i})}{\partial s_{i}} \dot{s}_{i} + \frac{\partial h_{i}(s_{i}, s_{\mathrm{d},i})}{\partial s_{\mathrm{d},i}} \dot{s}_{\mathrm{d},i} \right) \tilde{s}_{i} + h_{i}(s_{i}, s_{\mathrm{d},i}) \dot{\tilde{s}}_{i} \right]
= h_{i}(s_{i}, s_{\mathrm{d},i})\tilde{s}_{i} \left[\mu_{i}(s_{i}, s_{\mathrm{d},i}) \dot{\tilde{s}}_{i} + \tilde{s}_{i} \left(\frac{\partial h_{i}(s_{i}, s_{\mathrm{d},i})}{\partial s_{\mathrm{d},i}} + \frac{\partial h_{i}(s_{i}, s_{\mathrm{d},i})}{\partial s_{i}} \right) \dot{s}_{\mathrm{d},i} \right]
= -\gamma_{i} h_{i}^{2}(s_{i}, s_{\mathrm{d},i}) \tilde{s}_{i}^{2}.$$
(35)

To show i), let $(s_i, s_{d,i}) \in \mathcal{S}_i \times \mathcal{S}_{d,i}$, and (12) implies

$$h_i(s_i, s_{d,i}) \ge \frac{(\bar{s}_i - \underline{s}_i - \varepsilon_d)\varepsilon_d}{(\bar{s}_i - s_i)(s_i - \underline{s}_i)}.$$
(36)

Furthermore, since the denominator of (36) is maximized over $s_i \in \mathcal{S}_i$ at $s_i = (\underline{s}_i + \overline{s}_i)/2$, it follows that $h_i(s_i, s_{d,i}) \geq \underline{h}_i$, which together with (35) confirms i).

To show ii), since $s_i(0) \in \mathcal{S}_i$ and $s_{\mathrm{d},i}(0) \in \mathcal{S}_{\mathrm{d},i}$, it follows from (12) and (33) that $Z_i(\tilde{s}_i(0), s_{\mathrm{d},i}(0))$ is finite. Since, in addition, (35) implies that $Z_i(\tilde{s}_i, s_{\mathrm{d},i})$ is nonincreasing along (32), it follows that for all $t \geq 0$, $Z_i(\tilde{s}_i(t), s_{\mathrm{d},i}(t)) \leq Z_i(\tilde{s}_i(0), s_{\mathrm{d},i}(0)) < \infty$. Assume for contradiction that (O4) is not satisfied, which implies that there exists $t_1 > 0$ such that $s_i(t_1) = \bar{s}_i$ or $s_i(t_1) = \underline{s}_i$. Since, in addition, for all $t \geq 0$, $s_{\mathrm{d},i}(t) \in \mathcal{S}_{\mathrm{d},i}$, it follows from (12) and (33) that $Z_i(\tilde{s}_i(t_1), s_{\mathrm{d},i}(t_1)) = \infty$, which is a contradiction. Thus, for all $t \geq 0$, $s_i(t) \in \mathcal{S}_i$, which confirms ii).

To show iii), since for all $t \geq 0$, $(s_i(t), s_{d,i}(t)) \in \mathcal{S}_i \times \mathcal{S}_{d,i}$, it follows from i) that $\dot{Z}_i(\tilde{s}_i(t), s_{d,i}(t)) \leq -\gamma_i \underline{h}_i^2 \tilde{s}_i^2(t)$. Thus, LaSalle's invariance theorem implies that $\lim_{t\to\infty} \tilde{s}_i(t) = 0$, which confirms iii).

4.3. Orientation Kinematics

In this section, we examine the orientation kinematics (3) and the associated control (16). Define the desired pointing direction

$$b_{\mathrm{d},i} \triangleq \frac{1}{s_{\mathrm{d},i}} p_{\mathrm{d},i},$$

and note that Proposition 1 implies that for all $t \ge 0$, $s_{d,i}(t) > 0$, which implies that $b_{d,i}$ is well defined. Define the pointing direction error

$$\tilde{b}_i \triangleq R_i v_i - b_{\mathrm{d},i},$$

and note that for all $t \geq 0$, $\tilde{b}_i(t) \in \mathcal{B}_2$, where $\mathcal{B}_2 \triangleq \{b \in \mathbb{R}^m : ||b|| \leq 2\}$, which is the closed ball of radius 2. Differentiating \tilde{b}_i and using (3) and (16) implies

$$\dot{\tilde{b}}_i = \eta_i s_{\mathrm{d},i} \left(p_{\mathrm{d},i} v_i^{\mathrm{T}} v_i - R_i v_i p_{\mathrm{d},i}^{\mathrm{T}} R_i v_i \right) + \frac{1}{s_{\mathrm{d},i}^2} \left(\dot{p}_{\mathrm{d},i} p_{\mathrm{d},i}^{\mathrm{T}} - p_{\mathrm{d},i} \dot{p}_{\mathrm{d},i}^{\mathrm{T}} \right) R_i v_i - \dot{b}_{\mathrm{d},i}.$$

Since $p_{d,i} = s_{d,i}b_{d,i}$, $\dot{p}_{d,i} = \dot{s}_{d,i}b_{d,i} + s_{d,i}\dot{b}_{d,i}$, $v_i^Tv_i = 1$, and $b_{d,i} = -\tilde{b}_i + R_iv_i$, it follows that

$$\dot{\tilde{b}}_i = \eta_i s_{\mathrm{d},i}^2 \left(-\tilde{b}_i + \left(1 - b_{\mathrm{d},i}^\mathrm{T} R_i v_i \right) R_i v_i \right) - \dot{b}_{\mathrm{d},i} \left(1 - b_{\mathrm{d},i}^\mathrm{T} R_i v_i \right) - b_{\mathrm{d},i} \dot{b}_{\mathrm{d},i}^\mathrm{T} R_i v_i.$$

Since $b_{d,i}$ is a unit vector, it follows that $\dot{b}_{d,i}^{T}b_{d,i}=0$. In addition, note that $1-b_{d,i}^{T}R_{i}v_{i}=\frac{1}{2}\tilde{b}_{i}^{T}\tilde{b}_{i}$ and $R_{i}v_{i}=\tilde{b}_{i}+b_{d,i}$. Thus,

$$\dot{\tilde{b}}_i = -\eta_i s_{\mathrm{d},i}^2 \left(\tilde{b}_i - \frac{1}{2} \tilde{b}_i^{\mathrm{T}} \tilde{b}_i \left(\tilde{b}_i + b_{\mathrm{d},i} \right) \right) - \frac{1}{2} \dot{b}_{\mathrm{d},i} \tilde{b}_i^{\mathrm{T}} \tilde{b}_i - b_{\mathrm{d},i} \dot{b}_{\mathrm{d},i}^{\mathrm{T}} \tilde{b}_i.$$

$$(37)$$

Consider the Lyapunov-like function $W_i: \mathcal{B}_2 \to [0,2]$ defined by

$$W_i(\tilde{b}_i) \triangleq \frac{1}{2} \tilde{b}_i^{\mathrm{T}} \tilde{b}_i = 1 - b_{\mathrm{d},i}^{\mathrm{T}} R_i v_i, \tag{38}$$

and define the Lyapunov-like derivative

$$\dot{W}_i(\tilde{b}_i) \triangleq \frac{\partial W_i(\tilde{b}_i)}{\partial \tilde{b}_i} \dot{\tilde{b}}_i. \tag{39}$$

Define $\mathcal{R}_i \triangleq \left\{ R \in SO(m) : b_{\mathbf{d},i}^{\mathrm{T}}(0)Rv_i \neq -1 \right\}$, which is the set of all orientations Rv_i except those where the angle from $\dot{q}_i(0)$ to Rv_i is exactly π rad.

The next result shows that W_i is nonincreasing along the trajectories of (37); and for almost all initial conditions, that is, for all $R_i(0) \in \mathcal{R}_i$, the angle from $\dot{q}_i(t)$ to $p_{\mathrm{d},i}(t)$ is bounded away from π rad for all $t \geq 0$.

Proposition 5. Consider the closed-loop dynamics (37), which consists of (3)–(10) and (16). Assume that (A1) is satisfied. Then, the following statements hold:

- i) For all $\tilde{b}_i \in \mathcal{B}_2$, $\dot{W}_i(\tilde{b}_i) = -\frac{1}{2}\eta_i s_{\mathrm{d},i}^2 \tilde{b}_i^{\mathrm{T}} \tilde{b}_i \left(1 + b_{\mathrm{d},i}^{\mathrm{T}} R_i v_i\right)$, which is nonpositive.
- ii) For all $R_i(0) \in \mathcal{R}_i$, there exists $\varepsilon_i > 0$ such that for all $t \ge 0$, $1 + b_{d,i}^T(t)R_i(t)v_i \ge \varepsilon_i$.

Proof. Evaluating (39) along the trajectories of (37) yields

$$\dot{W}_{i}(\tilde{b}_{i}) = -\eta_{i}s_{\mathrm{d},i}^{2}\tilde{b}_{i}^{\mathrm{T}}\tilde{b}_{i}\left(1 - \frac{1}{2}\tilde{b}_{i}^{\mathrm{T}}\left(\tilde{b}_{i} + b_{\mathrm{d},i}\right)\right) - \frac{1}{2}\tilde{b}_{i}^{\mathrm{T}}\dot{b}_{\mathrm{d},i}\tilde{b}_{i}^{\mathrm{T}}\tilde{b}_{i} - \tilde{b}_{i}^{\mathrm{T}}b_{\mathrm{d},i}\dot{b}_{\mathrm{d},i}^{\mathrm{T}}\tilde{b}_{i} = -\frac{1}{2}\eta_{i}s_{\mathrm{d},i}^{2}\tilde{b}_{i}^{\mathrm{T}}\tilde{b}_{i}\left(1 + b_{\mathrm{d},i}^{\mathrm{T}}R_{i}v_{i}\right)$$

which is nonpositive because $b_{\mathrm{d},i}^{\mathrm{T}}R_{i}v_{i}\geq-1$, thus confirming i).

To show ii), since $b_{\mathbf{d},i}^{\mathrm{T}}(0)R_i(0)v_i \neq -1$, it follows from (38) that $W_i(\tilde{b}_i(0)) = 1 - b_{\mathbf{d},i}^{\mathrm{T}}(0)R_i(0)v_i < 2$. Define $\varepsilon_i \triangleq 2 - W(\tilde{b}_i(0)) \in (0,2]$, and since W_i is nonincreasing along the trajectories of (37), it follows that for all $t \geq 0, 1 + b_{\mathbf{d},i}^{\mathrm{T}}(t)R_i(t)v_i = 2 - W(\tilde{b}_i(t)) \geq \varepsilon_i$, which confirms ii).

4.4. Full Closed-Loop Dynamics

We now analyze the full closed-loop dynamics (1)–(17). Since $s_i R_i v_i - p_{d,i} = \tilde{s}_i R_i v_i + s_{d,i} \tilde{b}_i$, it follows from (25) that

$$\dot{\phi} = -\left[(L+A) \otimes I_m \right] B(\phi)\phi - \sum_{i \in \mathcal{I}} \left[(L+A)d_i \otimes I_m \right] \left(\tilde{s}_i R_i v_i + s_{\mathrm{d},i} \tilde{b}_i \right). \tag{40}$$

The next theorem is the main result, which shows that $(\phi(t), \tilde{s}_1(t), \dots, \tilde{s}_n(t), \tilde{b}_1(t), \dots, \tilde{b}_n(t)) \equiv 0$ is an almost globally exponentially stable equilibrium of the closed-loop system (32), (37), and (40). More specifically, the equilibrium is Lyapunov stable, and for almost all initial conditions $(q_i(0), s_i(0), R_i(0)) \in \mathbb{R}^m \times S_i \times SO(m)$, the state $(\phi_i, \tilde{s}_i, \tilde{b}_i)$ converges to zero exponentially and (O1)–(O4) are satisfied. In fact, the only initial conditions for which the state is not guaranteed to converge to zero are those where the angle from $\dot{q}_i(0)$ to $p_{\mathbf{d},i}(0)$ is exactly π rad, that is, $R_i(0) \in SO(m) \setminus \mathcal{R}_i$. Note that topological constraints associated with SO(m)

prevent global asymptotic stability of the equilibrium using a continuous time-invariant control [36]. The proof of this main result relies on a Lyapunov function that is a weighted summation of the Lyapunov-like functions (26), (33), and (38), which are used in each of the previous three subsections.

Theorem 1. Consider the closed-loop dynamics (32), (37), and (40), which consists of (1)–(17). Assume that L+A is nonsingular and (A1) is satisfied. Then, $(\phi(t), \tilde{s}_1(t), \dots, \tilde{s}_n(t), \tilde{b}_1(t), \dots, \tilde{b}_n(t)) \equiv 0$ is a Lyapunov stable equilibrium of (32), (37), and (40). Furthermore, for all initial conditions $(q_i(0), s_i(0), R_i(0)) \in \mathbb{R}^m \times \mathcal{S}_i \times \mathcal{R}_i$, the following statements hold:

- i) ϕ_i , \tilde{s}_i , \tilde{b}_i and ζ_i converge to zero exponentially.
- ii) (O1)-(O4) are satisfied.

Proof. Since D is diagonal, it follows from (26), (27), and (22) that

$$\dot{V}_0(\phi_1, \dots, \phi_n) = 2 \sum_{i \in \mathcal{I}} k_i d_i^{\mathrm{T}} D d_i \sigma(\|\phi_i\|^2) \phi_i^{\mathrm{T}} \dot{\phi}_i = 2\phi^{\mathrm{T}} B(\phi) \Big(D \otimes I_m \Big) \dot{\phi}. \tag{41}$$

Evaluating (41) along (40) yields

$$\dot{V}_{0}(\phi_{1}, \dots, \phi_{n}) = -\phi^{T} B(\phi) \Big[\Big((L+A)^{T} D + D(L+A) \Big) \otimes I_{m} \Big] B(\phi) \phi \\
- 2 \sum_{i \in \mathcal{I}} \phi^{T} B(\phi) \Big[D(L+A) d_{i} \otimes I_{m} \Big] \Big(\tilde{s}_{i} R_{i} v_{i} + s_{d,i} \tilde{b}_{i} \Big) \\
= -\phi^{T} B(\phi) (P \otimes I_{m}) B(\phi) \phi - 2 \sum_{i \in \mathcal{I}} \phi^{T} B(\phi) Q^{T} \Big(d_{i} \otimes I_{m} \Big) \Big(\tilde{s}_{i} R_{i} v_{i} + s_{d,i} \tilde{b}_{i} \Big), \tag{42}$$

where $P \triangleq (L+A)^{\mathrm{T}}D + D(L+A)$ and $Q \triangleq (L+A)^{\mathrm{T}}D \otimes I_m$. Since L+A is nonsingular, it follows from Lemma 2 that P is positive definite. Since L+A and D are nonsingular, it follows that Q is nonsingular. Thus,

$$c_1 \triangleq \frac{4n\lambda_{\max}(Q^{\mathrm{T}}Q)}{\lambda_{\min}(P)} > 0. \tag{43}$$

Next, note that

$$0 \le \left(\frac{1}{\sqrt{c_1}}QB(\phi)\phi + \sqrt{c_1}\tilde{s}_i(d_i \otimes I_m)R_iv_i\right)^{\mathrm{T}} \left(\frac{1}{\sqrt{c_1}}QB(\phi)\phi + \sqrt{c_1}\tilde{s}_i(d_i \otimes I_m)R_iv_i\right),$$

which implies that

$$-2\tilde{s}_i\phi^{\mathrm{T}}B(\phi)Q^{\mathrm{T}}(d_i\otimes I_m)R_iv_i \leq \frac{1}{c_1}\phi^{\mathrm{T}}B(\phi)Q^{\mathrm{T}}QB(\phi)\phi + c_1\tilde{s}_i^2.$$
(44)

Similarly,

$$-2s_{\mathrm{d},i}\phi^{\mathrm{T}}B(\phi)Q^{\mathrm{T}}(d_{i}\otimes I_{m})\tilde{b}_{i}\leq \frac{1}{c_{1}}\phi^{\mathrm{T}}B(\phi)Q^{\mathrm{T}}QB(\phi)\phi+c_{1}s_{\mathrm{d},i}^{2}\tilde{b}_{i}^{\mathrm{T}}\tilde{b}_{i}.$$
(45)

Substituting (44) and (45) into (42) and using (43) and (22) yields

$$\dot{V}_{0}(\phi_{1},\ldots,\phi_{n}) \leq -\phi^{T}B(\phi)(P\otimes I_{m})B(\phi)\phi + \sum_{i\in\mathcal{I}}\left(\frac{2}{c_{1}}\phi^{T}B(\phi)Q^{T}QB(\phi)\phi + c_{1}\left(\tilde{s}_{i}^{2} + s_{\mathrm{d},i}^{2}\tilde{b}_{i}^{T}\tilde{b}_{i}\right)\right)$$

$$\leq -\left(\lambda_{\min}(P) - \frac{2n\lambda_{\max}(Q^{T}Q)}{c_{1}}\right)\phi^{T}B^{2}(\phi)\phi + \sum_{i\in\mathcal{I}}c_{1}\left(\tilde{s}_{i}^{2} + s_{\mathrm{d},i}^{2}\tilde{b}_{i}^{T}\tilde{b}_{i}\right)$$

$$= -c_{2}\phi^{T}B^{2}(\phi)\phi + \sum_{i\in\mathcal{I}}c_{1}\left(\tilde{s}_{i}^{2} + s_{\mathrm{d},i}^{2}\tilde{b}_{i}^{T}\tilde{b}_{i}\right)$$

$$= \sum_{i\in\mathcal{I}}\left(-c_{2}k_{i}^{2}\sigma^{2}(\|\phi_{i}\|^{2})\phi_{i}^{T}\phi_{i} + c_{1}\left(\tilde{s}_{i}^{2} + s_{\mathrm{d},i}^{2}\tilde{b}_{i}^{T}\tilde{b}_{i}\right)\right).$$
(46)

where $c_2 \triangleq \lambda_{\min}(P)/2$.

To show that $(\phi(t), \tilde{s}_1(t), \dots, \tilde{s}_n(t), \tilde{b}_1(t), \dots, \tilde{b}_n(t)) \equiv 0$ is a Lyapunov stable equilibrium of (32), (37), and (40), consider the Lyapunov function $V : \mathbb{R}^m \times \dots \times \mathbb{R}^m \times \mathcal{S}_1 \times \dots \times \mathcal{S}_n \times \mathcal{B}_2 \times \dots \times \mathcal{B}_2 \times \mathcal{S}_{d,1} \times \dots \times \mathcal{S}_{d,n} \rightarrow [0, \infty)$ defined by

$$V(\phi_1, \dots, \phi_n, \tilde{s}_1, \dots, \tilde{s}_n, \tilde{b}_1, \dots, \tilde{b}_n, s_{d,1}, \dots, s_{d,n}) \triangleq V_0(\phi_1, \dots, \phi_n) + \sum_{i \in \mathcal{I}} \left(\frac{2c_1}{\underline{h}_i^2 \gamma_i} Z_i(\tilde{s}_i, s_{d,i}) + \frac{4c_1}{\bar{\varepsilon}_i \eta_i} W_i(\tilde{b}_i) \right), \tag{47}$$

where $\bar{\varepsilon}_i \in (0,2)$, and $\underline{h}_i > 0$ is given by i) of Proposition 4. Using i) of Proposition 4, i) of Proposition 5, and (46) to evaluate V along the trajectories of (32), (37), and (40) yields

$$\dot{V} \triangleq \dot{V}_{0}(\phi_{1}, \dots, \phi_{n}) + \sum_{i \in \mathcal{I}} \left(\frac{2c_{1}}{\underline{h}_{i}^{2} \gamma_{i}} \dot{Z}_{i}(\tilde{s}_{i}, s_{\mathrm{d}, i}) + \frac{4c_{1}}{\bar{\varepsilon}_{i} \eta_{i}} \dot{W}_{i}(\tilde{b}_{i}) \right) \\
\leq - \sum_{i \in \mathcal{I}} \left(c_{2} k_{i}^{2} \sigma^{2} (\|\phi_{i}\|^{2}) \phi_{i}^{\mathrm{T}} \phi_{i} + c_{1} \tilde{s}_{i}^{2} + c_{1} \left(\frac{2(1 + b_{\mathrm{d}, i}^{\mathrm{T}} R_{i} v_{i})}{\bar{\varepsilon}_{i}} - 1 \right) s_{\mathrm{d}, i}^{2} \tilde{b}_{i}^{\mathrm{T}} \tilde{b}_{i} \right), \tag{48}$$

where we omit the arguments from \dot{V} . Define $r \triangleq 4 - \bar{\varepsilon}_i > 0$ and $B_r \triangleq \{\tilde{b}_i \in \mathbb{R}^m : \tilde{b}_i^{\mathrm{T}} \tilde{b}_i < r\}$. Since $1 + b_{\mathrm{d},i}^{\mathrm{T}} R_i v_i = 2 - \tilde{b}_i^{\mathrm{T}} \tilde{b}_i / 2$, it follows from (48) that for all $(\phi_i, \tilde{s}_i, \tilde{b}_i, s_{\mathrm{d},i}) \in \mathbb{R}^m \times \mathcal{S}_i \times B_r \times \mathcal{S}_{\mathrm{d},i}, \dot{V} \leq -\sum_{i \in \mathcal{I}} (c_2 k_i^2 \sigma^2(\|\phi_i\|^2) \phi_i^{\mathrm{T}} \phi_i + c_1 \tilde{s}_i^2)$, which is nonpositive. Thus, the origin is a Lyapunov stable equilibrium. To show i), consider (47) with $\bar{\varepsilon}_i = \varepsilon_i$, where $\varepsilon_i > 0$ is given by ii) of Proposition 5. Thus, it follows from (48), ii) of Proposition 5, and Proposition 1 that for all $t \geq 0$,

$$\dot{V}(t) \leq -\sum_{i \in \mathcal{I}} \left(c_2 k_i^2 \sigma^2 (\|\phi_i(t)\|^2) \|\phi_i(t)\|^2 + c_1 \tilde{s}_i^2(t) + c_1 s_{\mathrm{d},i}^2(t) \|\tilde{b}_i(t)\|^2 \right) \\
\leq -\sum_{i \in \mathcal{I}} \left(c_2 k_i^2 \sigma^2 (\|\phi_i(t)\|^2) \|\phi_i(t)\|^2 + c_1 \tilde{s}_i^2(t) + c_1 \underline{s}_i^2 \|\tilde{b}_i(t)\|^2 \right),$$

which implies that V is nonincreasing. Since, in addition, V is radially unbounded, it follows that ϕ_i is bounded, which implies that there exists $\sigma_{\min} > 0$ such that for all $t \ge 0$, $\sigma(\|\phi_i(t)\|^2) > \sigma_{\min}$. Thus,

$$\dot{V}(t) \le -\sum_{i \in \mathcal{I}} \left(c_2 k_i^2 \sigma_{\min}^2 \|\phi_i(t)\|^2 + c_1 \tilde{s}_i^2(t) + c_1 \underline{s}_i^2 \|\tilde{b}_i(t)\|^2 \right). \tag{49}$$

Next, note that $\nu_1 + \nu_2 \|\phi_i\|^2 \le \nu_1 + 2\nu_2 \|\phi_i\|^2 + \frac{\nu_2^2}{\nu_1} \|\phi_i\|^4 = (\sqrt{\nu_1} + \frac{\nu_2}{\sqrt{\nu_1}} \|\phi_i\|^2)^2$, and taking the square root of each side implies that

$$\sqrt{\nu_1 + \nu_2 \|\phi_i\|^2} - \sqrt{\nu_1} \le \frac{\nu_2}{\sqrt{\nu_1}} \|\phi_i\|^2. \tag{50}$$

Together, (26) and (50) imply that

$$V_0(\phi_1, \dots, \phi_n) \le \frac{2}{\sqrt{\nu_1}} \sum_{i \in \mathcal{I}} k_i d_i^{\mathrm{T}} D d_i \|\phi_i\|^2 \le c_3 \sum_{i \in \mathcal{I}} k_i^2 \|\phi_i\|^2,$$
 (51)

where $c_3 \triangleq \max_{i \in \mathcal{I}} 2d_i^{\mathrm{T}} Dd_i/(k_i\sqrt{\nu_1})$. Next, ii) and iii) of Proposition 4 implies that for all $t \geq 0$, $s_i(t) \in \mathcal{S}_i$ and that $\lim_{t \to \infty} \tilde{s}_i(t) = 0$. Since, in addition, for all $t \geq 0$, $s_{\mathrm{d},i}(t) \in \mathcal{S}_{\mathrm{d},i}$, it follows from (12) that there exists $\bar{h}_i > 0$ such that for all $t \geq 0$, $h_i(s_i(t), s_{\mathrm{d},i}(t)) \leq \bar{h}_i$. Thus, (33) implies that for all $t \geq 0$,

$$Z_i(\tilde{s}_i(t), s_{d,i}(t)) \le \frac{\bar{h}_i^2}{2} \tilde{s}_i^2. \tag{52}$$

Therefore, combining (38), (51), and (52) with (49) yields

$$\dot{V}(t) \leq -\frac{c_2 \sigma_{\min}^2}{c_3} V_0(\phi_1(t), \dots, \phi_n(t)) - \sum_{i \in \mathcal{I}} \left(\frac{2c_1}{\bar{h}_i^2} Z_i(\tilde{s}_i(t), s_{\mathrm{d},i}(t)) + 2c_1 \underline{s}_i^2 W_i(\tilde{b}_i(t)) \right),$$

and using (47) yields

$$\dot{V}(t) \le -c_4 V(\phi_1(t), \dots, \phi_n(t), \tilde{s}_1(t), \dots, \tilde{s}_n(t), \tilde{b}_1(t), \dots, \tilde{b}_n(t), s_{d,1}(t), \dots, s_{d,n}(t)),$$

where $c_4 \triangleq \min\{\frac{c_2\sigma_{\min}^2}{c_3}, \frac{h_1^2\gamma_1}{\tilde{h}_1^2}, \dots, \frac{h_n^2\gamma_n}{h_n^2}, \frac{\bar{\epsilon}_1\eta_1s_1^2}{2}, \dots, \frac{\bar{\epsilon}_n\eta_ns_n^2}{2}\}$ is positive. Thus, $V(t) \leq e^{-c_4t}V(0)$, which implies that V converges to zero exponentially. Therefore, each term in (47) converges to zero exponentially, which implies that V_0 , Z_i , and W_i converge to zero exponentially. Since V_0 converges to zero exponentially, (26) implies that ϕ_i converges to zero exponentially. Since, in addition, L+A is nonsingular, it follows from (20) that ζ_i converges to zero exponentially. Next, since for all $t \geq 0$, $(s_i(t), s_{\mathrm{d},i}(t)) \in \mathcal{S}_i \times \mathcal{S}_{\mathrm{d},i}$, it follows that $h_i(s_i(t), s_{\mathrm{d},i}(t)) \geq h_i$. Since, in addition, Z_i converges to zero exponentially, (33) implies that \tilde{s}_i converges to zero exponentially. Finally, since W_i converges to zero exponentially, (38) implies that \tilde{b}_i converges to zero exponentially, which confirms i).

To show ii), since $\lim_{t\to\infty} \zeta_i(t) = 0$ and R_g is bounded, it follows that (O3) is satisfied, which implies that (O1) is satisfied. Next, since $s_{d,i}$ is bounded, $\lim_{t\to\infty} \phi(t) = 0$, $\lim_{t\to\infty} \tilde{s}_i(t) = 0$, and $\lim_{t\to\infty} \tilde{b}_i = 0$, it follows from (40) that $\lim_{t\to\infty} \dot{\phi}(t) = 0$. Since, in addition, L + A is nonsingular, it follows from (24) that $\lim_{t\to\infty} \dot{\zeta}(t) = 0$, which confirms (O2). Lastly, (O4) follows from ii) of Proposition 4.

Next, we present two specializations of Theorem 1, which address the cases where either the speed s_i or the pointing direction $R_i v_i$ are control variables. The proofs of these results are similar to the proof of Theorem 1. Note that Proposition 3 addresses the case where both speed s_i and the pointing direction $R_i v_i$ are control variables.

Theorem 2. Consider the closed-loop dynamics (37) and (40), which consists of (1), (3)–(10), and (16), where $s_i = s_{d,i}$. Assume that L + A is nonsingular and (A1) is satisfied. Then, $(\phi(t), \tilde{b}_1(t), \dots, \tilde{b}_n(t)) \equiv 0$ is a Lyapunov stable equilibrium of (37) and (40) with $s_i = s_{d,i}$. Furthermore, for all initial conditions $(q_i(0), R_i(0)) \in \mathbb{R}^m \times \mathcal{R}_i$, ϕ_i , \tilde{b}_i , and ζ_i converge to zero exponentially, and (O1)–(O4) are satisfied.

Theorem 3. Consider the closed-loop dynamics (32) and (40), which consists of (1), (2), (4)–(15), and (17), where $R_i v_i = b_{d,i}$. Assume that L + A is nonsingular and (A1) is satisfied. Then, $(\phi(t), \tilde{s}_1(t), \dots, \tilde{s}_n(t)) \equiv 0$ is a Lyapunov stable equilibrium of (32) and (40) with $R_i v_i = b_{d,i}$. Furthermore, for all initial conditions $(q_i(0), s_i(0)) \in \mathbb{R}^m \times \mathcal{S}_i$, ϕ_i , \tilde{s}_i , and ζ_i converge to zero exponentially, and (O1)–(O4) are satisfied.

5. Adaptive Formation Control Algorithm with Uncertainty in Speed Dynamics

In this section, we extended the formation control (4)–(17) to address uncertainty in the speed dynamics (2), specifically, uncertainty in $f_i(s_i, R_i)$ and $g_i(s_i, R_i)$, which appear in (2). We develop and analyze an adaptive controller, which is used in place of the non-adaptive controller (15). First, the functions $f_i(s_i, R_i)$ and $g_i(s_i, R_i)$ are parameterized as

$$f_i(s_i, R_i) = \chi_{*,i}^{\mathrm{T}} \Gamma_i(s_i, R_i), \tag{53}$$

$$q_i(s_i, R_i) = r_{*,i} \psi_i(s_i, R_i),$$
 (54)

where $\Gamma_i : \mathcal{S}_i \times \mathrm{SO}(m) \to \mathbb{R}^{n_i}$ and $\psi_i : \mathcal{S}_i \times \mathrm{SO}(m) \to \mathbb{R} \setminus \{0\}$ are continuous, $\chi_{*,i} \in \mathbb{R}^{n_i}$, and $r_{*,i} \neq 0$. We assume that Γ_i and ψ_i are known, and the sign of $r_{*,i}$ is known; however, $\chi_{*,i}$ and $|r_{*,i}|$ are unknown. Without loss of generality, let $r_{*,i} > 0$ and $\psi_i : \mathcal{S}_i \times \mathrm{SO}(m) \to (0,\infty)$.

The adaptive approach in this section uses the continuous projection operator. Here, we briefly review this operator. For more details, see [41, Appendix E]. To define the continuous projection operator, let $w: \mathbb{R}^{\ell_w} \to \mathbb{R}$ be a continuously differentiable convex function, and consider $\nabla w: \mathbb{R}^{\ell_w} \to \mathbb{R}^{\ell_w}$ defined by

 $\nabla w(x) \triangleq \left[\partial w(x)/\partial x\right]^{\mathrm{T}}$. Let $\varepsilon_{\mathrm{p}} > 0$ and let $M \in \mathbb{R}^{\ell_w \times \ell_w}$ be positive definite, and consider the continuous projection operator $\mathrm{Proj}_{w,M} \colon \mathbb{R}^{\ell_w} \times \mathbb{R}^{\ell_w} \to \mathbb{R}^{\ell_w}$ defined by

$$\operatorname{Proj}_{w,M}(x,y) \triangleq \begin{cases} y - \min \Big\{ 1, \frac{w(x)}{\varepsilon_{\operatorname{p}}} \Big\} M \nabla w(x) \frac{\nabla w^{\operatorname{T}}(x) y}{\nabla w^{\operatorname{T}}(x) M \nabla w(x)}, & w(x) \geq 0 \text{ and } y^{\operatorname{T}} \nabla w(x) > 0, \\ y, & \text{otherwise.} \end{cases}$$

Define the unknown system parameters $\theta_{*,i} \triangleq \chi_{*,i}/r_{*,i} \in \mathbb{R}^{n_i}$ and $l_{*,i} \triangleq 1/r_{*,i} > 0$. Next, let $w_i : \mathbb{R}^{n_i} \to \mathbb{R}$ be a continuously differentiable convex function, and define $\Theta_i \triangleq \{\theta \in \mathbb{R}^{n_i} : w_i(\theta) \leq 0\}$, which is convex and assumed to be such that $\theta_{*,i} \in \Theta_i$. Similarly, let $z_i : \mathbb{R} \to \mathbb{R}$ be a continuously differentiable convex function, and define $L_i \triangleq \{l \in \mathbb{R} : z_i(l) \leq 0\}$, which is convex and assumed to be such that $l_{*,i} \in L_i$. Lastly, define $\bar{\Theta}_i \triangleq \{\theta \in \mathbb{R}^{n_i} : w_i(\theta) \leq \varepsilon_p\}$ and $\bar{L}_i \triangleq \{l \in \mathbb{R} : z_i(l) \leq \varepsilon_p\}$, which are convex supersets of Θ_i and L_i , respectively.

Let $\gamma_i > 0$, and consider the formation controller (4)–(14), (16), and (17) combined with the adaptive speed controller

$$u_{i} = \frac{-1}{\psi_{i}(s_{i}, R_{i})} \left(\theta_{i}^{T} \Gamma_{i}(s_{i}, R_{i}) + \frac{\gamma_{i}(s_{i} - s_{d,i}) h_{i}(s_{i}, s_{d,i})}{\mu_{i}(s_{i}, s_{d,i})} + \frac{l_{i} \dot{s}_{d,i} \upsilon_{i}(s_{i}, s_{d,i})}{\mu_{i}(s_{i}, s_{d,i})} \right),$$
(55)

where $v_i: \mathcal{S}_i \times \mathcal{S}_{d_i} \to \mathbb{R}$ is defined by

$$v_i(s_i, s_{d,i}) \triangleq (s_i - s_{d,i}) \frac{\partial h_i(s_i, s_{d,i})}{\partial s_{d,i}} - h_i(s_i, s_{d,i}), \tag{56}$$

and the adaptive parameters $\theta_i:[0,\infty)\to\bar{\Theta}_i$ and $l_i:[0,\infty)\to\bar{L}_i$ satisfy

$$\dot{\theta}_i = \operatorname{Proj}_{w_i, M_i} \Big(\theta_i, (s_i - s_{d,i}) h_i(s_i, s_{d,i}) \mu_i(s_i, s_{d,i}) M_i \Gamma_i(s_i, R_i) \Big), \tag{57}$$

$$\dot{l}_i = \operatorname{Proj}_{z_i, \tau_i} \left(l_i, \tau_i(s_i - s_{d,i}) h_i(s_i, s_{d,i}) v_i(s_i, s_{d,i}) \dot{s}_{d,i} \right), \tag{58}$$

where $\theta_i(0) \in \bar{\Theta}_i$, $l_i(0) \in \bar{L}_i$, $\tau_i > 0$, and $M_i \in \mathbb{R}^{n_i \times n_i}$ is positive definite. Note that if $l_i = l_{*,i}$ and $\theta_i = \theta_{*,i}$, then (55) and (56) are equivalent to the non-adaptive speed control (15), where the gain γ_i in (15) is replaced by $\gamma_i/r_{*,i}$. We also note that the adaptive laws (57) and (58) can be modified using standard robust modification methods (e.g., normalization, dead-zone, e-modification); see [42] for more details.

To analyze closed-loop stability, define the parameter estimation errors

$$\tilde{\theta}_i \triangleq \theta_i - \theta_{*,i}, \qquad \tilde{l}_i \triangleq l_i - l_{*,i}.$$

Differentiating \tilde{s}_i and using (2) and (53)–(56) yields

$$\dot{\tilde{s}}_{i} = \chi_{*,i}^{T} \Gamma_{i}(s_{i}, R_{i}) - r_{*,i} \left(\theta_{i}^{T} \Gamma_{i}(s_{i}, R_{i}) + \frac{\gamma_{i} \tilde{s}_{i} h_{i}(s_{i}, s_{d,i})}{\mu_{i}(s_{i}, s_{d,i})} + \frac{l_{i} \dot{s}_{d,i} v_{i}(s_{i}, s_{d,i})}{\mu_{i}(s_{i}, s_{d,i})} \right) - \dot{s}_{d,i}$$

$$= -r_{*,i} \tilde{\theta}_{i}^{T} \Gamma_{i}(s_{i}, R_{i}) - \frac{r_{*,i}}{\mu_{i}(s_{i}, s_{d,i})} \left[\gamma_{i} \tilde{s}_{i} h_{i}(s_{i}, s_{d,i}) + \tilde{l}_{i} \dot{s}_{d,i} v_{i}(s_{i}, s_{d,i}) \right] - \left[\frac{v_{i}(s_{i}, s_{d,i})}{\mu_{i}(s_{i}, s_{d,i})} + 1 \right] \dot{s}_{d,i}. \tag{59}$$

Consider the Lyapunov-like function $Z_i: S_i \times S_{d,i} \times \bar{\Theta}_i \times \bar{L}_i$ defined by

$$Z_{i}(\tilde{s}_{i}, s_{d,i}, \tilde{\theta}_{i}, \tilde{l}_{i}) \triangleq \frac{1}{2r_{*,i}} h_{i}^{2}(s_{i}, s_{d,i}) \tilde{s}_{i}^{2} + \frac{1}{2} \tilde{\theta}_{i}^{T} M_{i}^{-1} \tilde{\theta}_{i} + \frac{1}{2\tau_{i}} \tilde{l}_{i}^{2}, \tag{60}$$

and define the Lyapunov-like derivative

$$\dot{Z}_{i}(\tilde{s}_{i}, s_{\mathrm{d},i}, \tilde{\theta}_{i}, \tilde{l}_{i}) \triangleq \frac{\partial Z_{i}(\tilde{s}_{i}, s_{\mathrm{d},i}, \tilde{\theta}_{i}, \tilde{l}_{i})}{\partial \tilde{s}_{i}} \dot{\tilde{s}}_{i} + \frac{\partial Z_{i}(\tilde{s}_{i}, s_{\mathrm{d},i}, \tilde{\theta}_{i}, \tilde{l}_{i})}{\partial \tilde{s}_{\mathrm{d},i}} \dot{s}_{\mathrm{d},i} + \frac{\partial Z_{i}(\tilde{s}_{i}, s_{\mathrm{d},i}, \tilde{\theta}_{i}, \tilde{l}_{i})}{\partial \tilde{\theta}_{i}} \dot{\theta}_{i} + \frac{\partial Z_{i}(\tilde{s}_{i}, s_{\mathrm{d},i}, \tilde{\theta}_{i}, \tilde{l}_{i})}{\partial \tilde{l}_{i}} \dot{l}_{i}.$$
(61)

The next result shows that if (A1) is satisfied, $s_i(0) \in \mathcal{S}_i$, $\theta_i(0) \in \bar{\Theta}_i$, and $l_i(0) \in \bar{L}_i$, then for all $t \geq 0$, $s_i(t) \in \mathcal{S}_i$, $\theta_i(t) \in \bar{\Theta}_i$, and $l_i(t) \in \bar{L}_i$, and $\lim_{t \to \infty} \tilde{s}_i(t) = 0$.

Proposition 6. Consider the closed-loop dynamics (57)–(59), which consists of (2), (4)–(14), (17), and (53)–(58). Assume that (A1) is satisfied. Then, the following statements hold:

- i) For all $(s_i, s_{d,i}, \theta_i, l_i) \in \mathcal{S}_i \times \mathcal{S}_{d,i} \times \bar{\Theta}_i \times \bar{L}_i$, $\dot{Z}_i(s_i, s_{d,i}, \tilde{\theta}_i, \tilde{l}_i) = -\gamma_i h_i^2(s_i, s_{d,i}) \tilde{s}_i^2 \leq -\gamma_i \underline{h}_i^2 \tilde{s}_i^2$, where $\underline{h}_i \triangleq \frac{4(\bar{s}_i \underline{s}_i \varepsilon_d)\varepsilon_d}{(\bar{s}_i \underline{s}_i)^2} > 0$.
- ii) For all $(s_i(0), \theta_i(0), l_i(0)) \in \mathcal{S}_i \times \bar{\Theta}_i \times \bar{L}_i$, (O4) is satisfied.
- iii) For all $(s_i(0), \theta_i(0), l_i(0)) \in S_i \times \bar{\Theta}_i \times \bar{L}_i$, $\lim_{t \to \infty} \tilde{s}_i(t) = 0$.
- iv) For all $(s_i(0), \theta_i(0), l_i(0)) \in S_i \times \bar{\Theta}_i \times \bar{L}_i$ and for all $t \geq 0$, $\theta_i(t) \in \bar{\Theta}_i$ and $l_i(t) \in \bar{L}_i$.

Proof. Computing the partial derivatives in (61) and using (17) and (56) yields

$$\dot{Z}_{i}(\tilde{s}_{i}, s_{\mathrm{d},i}, \tilde{\theta}_{i}, \tilde{l}_{i}) = \frac{h_{i}(s_{i}, s_{\mathrm{d},i})\tilde{s}_{i}}{r_{*,i}} \left[\left(\frac{\partial h_{i}(s_{i}, s_{\mathrm{d},i})}{\partial s_{i}} \dot{s}_{i} + \frac{\partial h_{i}(s_{i}, s_{\mathrm{d},i})}{\partial s_{\mathrm{d},i}} \dot{s}_{\mathrm{d},i} \right) \tilde{s}_{i} + h_{i}(s_{i}, s_{\mathrm{d},i}) \dot{\tilde{s}}_{i} \right] + \tilde{\theta}_{i}^{\mathrm{T}} M_{i}^{-1} \dot{\theta}_{i} + \frac{\tilde{l}_{i} \dot{l}_{i}}{\tau_{i}} \\
= \frac{h_{i}(s_{i}, s_{\mathrm{d},i})\tilde{s}_{i}}{r_{*,i}} \left[\mu_{i}(s_{i}, s_{\mathrm{d},i}) \dot{\tilde{s}}_{i} + \left(v_{i}(s_{i}, s_{\mathrm{d},i}) + \mu_{i}(s_{i}, s_{\mathrm{d},i}) \right) \dot{s}_{\mathrm{d},i} \right] + \tilde{\theta}_{i}^{\mathrm{T}} M_{i}^{-1} \dot{\theta}_{i} + \frac{\tilde{l}_{i} \dot{l}_{i}}{\tau_{i}}, \tag{62}$$

and evaluating (62) along the trajectories of (57)–(59) yields

$$\dot{Z}_{i}(\tilde{s}_{i}, s_{\mathrm{d},i}, \tilde{\theta}_{i}, \tilde{l}_{i}) = -h_{i}(s_{i}, s_{\mathrm{d},i})\tilde{s}_{i} \left[\mu_{i}(s, s_{\mathrm{d},i})\tilde{\theta}_{i}^{\mathrm{T}}\Gamma_{i}(s_{i}, R_{i}) + \gamma_{i}\tilde{s}_{i}h_{i}(s_{i}, s_{\mathrm{d},i}) + \tilde{l}_{i}\dot{s}_{\mathrm{d},i}v_{i}(s_{i}, s_{\mathrm{d},i}) \right]
+ \tilde{\theta}_{i}^{\mathrm{T}}M_{i}^{-1}\operatorname{Proj}_{w_{i}, M_{i}} \left(\theta_{i}, \tilde{s}_{i}h_{i}(s_{i}, s_{\mathrm{d},i})\mu_{i}(s_{i}, s_{\mathrm{d},i})M_{i}\Gamma_{i}(s_{i}, R_{i}) \right)
+ \frac{\tilde{l}_{i}}{\tau_{i}}\operatorname{Proj}_{z_{i}, \tau_{i}} \left(l_{i}, \tau_{i}\tilde{s}_{i}h_{i}(s_{i}, s_{\mathrm{d},i})v_{i}(s_{i}, s_{\mathrm{d},i})\dot{s}_{\mathrm{d},i} \right).$$
(63)

Next, it follows from [41, Lemma E.1] that for all $y \in \mathbb{R}^{n_i}$, $\tilde{\theta}_i^{\mathrm{T}} M_i^{-1} \operatorname{Proj}_{w_i,M_i}(\theta_i,y) \leq \tilde{\theta}_i^{\mathrm{T}} M_i^{-1} y$, and for all $a \in \mathbb{R}$, $\tau_i^{-1} \tilde{l}_i \operatorname{Proj}_{z_i,\tau_i}(l_i,a) \leq \tau_i^{-1} \tilde{l}_i a$. Thus, (63) implies that $\dot{Z}_i(\tilde{s}_i,s_{\mathrm{d},i},\tilde{\theta}_i,\tilde{l}_i) = -\gamma_i h_i^2(s_i,s_{\mathrm{d},i})\tilde{s}_i^2$. Using the same steps that are used after (35) in the proof of Proposition 4, it follows that i)–iii) are satisfied. Lastly, iv) follows directly from [41, Lemma E.1].

The following theorem is the main result that addresses the case where the speed dynamics are uncertain and the adaptive speed controller (55)–(58) is used in place of the non-adaptive speed controller (15) in combination with the rest of the formation control algorithm (4)–(14), (16), and (17). This result shows that $(\phi(t), \tilde{s}_1(0), \ldots, \tilde{s}_n(t), \tilde{b}_1(t), \ldots, \tilde{b}_n(t), \tilde{\theta}_1(t), \ldots, \tilde{\theta}_n(t), \tilde{l}_1(t), \ldots, \tilde{l}_n(t)) \equiv 0$ is a Lyapunov stable equilibrium of the closed-loop system (37), (40), and (57)–(59), and for all $(q_i(0), s_i(0), R_i(0), \theta_i(0), l_i(0)) \in \mathbb{R}^m \times \mathcal{S}_i \times \mathcal{R}_i \times \bar{\Theta}_i \times \bar{L}_i$, (O1)–(O4) are satisfied. The proof is similar to the proof of Theorem 1 except (60) is used in place of (33) for Z_i , and Proposition 6 is used in place of Proposition 4.

Theorem 4. Consider the closed-loop dynamics (37), (40), and (57)–(59), which consists of (1)–(14), (16), (17), and (53)–(58). Assume that L+A is nonsingular and (A1) is satisfied. Then, $(\phi(t), \tilde{s}_1(0), \ldots, \tilde{s}_n(t), \tilde{b}_1(t), \ldots, \tilde{b}_n(t), \tilde{\theta}_1(t), \ldots, \tilde{\theta}_n(t), \tilde{l}_1(t), \ldots, \tilde{l}_n(t)) \equiv 0$ is a Lyapunov stable equilibrium of (37), (40), and (57)–(59). Furthermore, for all initial conditions $(q_i(0), s_i(0), R_i(0), \theta_i(0), l_i(0)) \in \mathbb{R}^m \times \mathcal{S}_i \times \mathcal{R}_i \times \bar{\theta}_i \times \bar{L}_i, \lim_{t \to \infty} \zeta_i(t) = 0$, $\lim_{t \to \infty} \tilde{s}_i(t) = 0$, and $\lim_{t \to \infty} \tilde{b}_i(t) = 0$; (O1)–(O4) are satisfied; and for all $t \geq 0$, $\theta_i(t) \in \bar{\theta}_i$ and $l_i(t) \in \bar{L}_i$.

Theorem 4 guarantees that $(\phi_i, \tilde{s}_i, \tilde{b}_i)$ converges to zero, and (O1)–(O4) are satisfied. Furthermore, the result shows that the adaptive parameters θ_i and l_i are bounded; however, these parameters are not

guaranteed to converge to the unknown values $\theta_{*,i}$ and $l_{*,i}$. The lack of guaranteed convergence for the adaptive parameters is common in adaptive control schemes, where the control objective (e.g., convergence of $(\phi_i, \tilde{s}_i, \tilde{b}_i)$ to zero) can be achieved without perfect parameter estimation. In order for θ_i and l_i to converge to $\theta_{*,i}$ and $l_{*,i}$, the regressors $\Gamma_i(s_i, s_{d,i})$ and $\dot{s}_{d,i}$ in the adaptive laws (57) and (58) must be sufficiently rich (i.e., sufficiently exciting), which, in turn, depends on the exogenous leader trajectory (i.e., q_g and R_g). For more information on adaptive parameter convergence, see [41, 43, 44] for a discussion of persistency of excitation.

Finally, we note that Theorem 4 specializes to the case where the pointing direction $R_i v_i$ is a control variable and the speed dynamics are uncertain; similar to how Theorem 1 specializes to Theorem 3.

6. Numerical Simulations

For all examples, let n=3 and m=3, and for $i \in \{1,2,3\}$, define $e_i \triangleq [0_{1\times i-1} \quad 1 \quad 0_{1\times 3-i}]^T \in \mathbb{R}^3$. Let $v_i = e_1$, which implies that each agent's velocity is in the body-fixed e_1 -direction. The speed bounds are $\underline{s}_i = 8$ m/s and $\overline{s}_i = 18$ m/s. Each agent's initial position $q_i(0)$ and initial orientation $R_i(0)$ are selected randomly, and each agent's initial speed $s_i(0)$ is selected randomly such that $s_i(0) \in \mathcal{S}_i$.

The leader position $q_{\rm g}$ and orientation $R_{\rm g}$ satisfy (1) and (3) with i replaced with ${\rm g}$, where $v_{\rm g}=e_1$, $s_{\rm g}=12~{\rm m/s},\ q_{\rm g}(0)=0~{\rm m},\ R_{\rm g}(0)=I_m$, and $\Omega_{\rm g}$ is the skew-symmetric form of the angular velocity vector $\begin{bmatrix} 0 & 0.1\cos 0.5\pi t & 0.1t + 0.2\cos \pi t \end{bmatrix}^{\rm T}$ rad/s. The desired relative positions are $\delta_1=\begin{bmatrix} -5 & 5 & 1 \end{bmatrix}^{\rm T}$ m, $\delta_2=\begin{bmatrix} -5 & -5 & 2 \end{bmatrix}^{\rm T}$ m, and $\delta_3=\begin{bmatrix} -10 & -10 & 3 \end{bmatrix}^{\rm T}$ m. Note that for all $t\geq 0$, $\|\dot{q}_{\rm g}(t)+R_{\rm g}(t)\delta_i\|\in(10.5,15.7)$. Thus, (A1) is satisfied with $\kappa_i=2.3$.

Let $\mathcal{N}_1 = \{3\}$, $\mathcal{N}_2 = \{1\}$, and $\mathcal{N}_3 = \{2\}$, which represents a cyclic feedback structure. For all $j \in \mathcal{N}_i$, let $\beta_{ij} = 0.6$. Let $\alpha_1 = 2$ and $\alpha_2 = \alpha_3 = 0$, which implies that only the first agent has access to a measurement of its position relative to the leader (i.e., $q_g - q_1$). The formation control is implemented with $\nu_1 = \nu_2 = 1$ and $k_i = 2$, which satisfies $k_i \in (0, \kappa_i \sqrt{\nu_2})$. Each agent's measurement of q_i , s_i , and the Euler angles that parameterize R_i are corrupted by additive zero-mean Gaussian white noise with intensities 2×10^{-6} m², 3×10^{-7} m²/s², and 5×10^{-6} rad², respectively.

The next two examples demonstrate the non-adaptive formation control (4)–(17).

Example 1. For this example, $f_i(s_i, R_i) = -s_i$ and $g_i(s_i, R_i) = 1$, which implies that the speed dynamics are low-pass and linear with unity gain at dc. We implement the (non-adaptive) formation control (4)–(17), where $\gamma_i = 1$ and and $\eta_i = 0.3$. Figure 1 shows the 3-dimensional trajectories of the leader and agents, and Figure 3 shows that $q_i - q_g$ approaches $R_g \delta_i$, which implies that the formation control objectives are satisfied. The relative positions converge to the desired values by approximately t = 20 s. The root mean square (RMS) of $\|\zeta_i\|$ from t = 30 s to t = 60 s is 0.00041 m, 0.00359 m, and 0.00193 m for agent 1, 2, and 3, respectively. Note that if the sensor noise is absent, then the RMS errors converge to zero as stated in Theorem 1. Figure 2 shows that s_i approaches $s_{d,i}$, and that s_i is inside the speed bounds for all time.

Example 2. For this example, $f_i(s_i, R_i) = -0.005 |s_i| s_i + g e_3^T R_i v_i$ and $g_i(s_i, R_i) = 0.5$, where $-|s_i| s_i$ models aerodynamic drag on the agent (e.g., aircraft) and $g e_3^T R_i v_i$ models the acceleration due to gravity $g = 9.81 \text{ m/s}^2$ that is in the direction of velocity. We implement the (non-adaptive) formation control (4)–(17), where $\gamma_i = 10$ and and $\eta_i = 0.3$. Figure 4 shows the 3-dimensional trajectories of the leader and agents, and Figure 6 shows that $q_i - q_g$ approaches $R_g \delta_i$, which implies that the formation control objectives are satisfied. The relative positions converge to the desired values by approximately t = 25 s. The RMS of $||\zeta_i||$ from t = 30 s to t = 60 s is 0.00045 m, 0.00306 m, and 0.00172 m for agent 1, 2, and 3, respectively. Figure 5 shows that s_i approaches $s_{d,i}$, and that s_i is inside the speed bounds for all time.

The next example demonstrates the adaptive formation control (4)–(14), (16), (17), and (55)–(58).

Example 3. For this example, $f_i(s_i, R_i) = -0.005 |s_i| s_i + g e_3^{\mathrm{T}} R_i v_i$ and $g_i(s_i, R_i) = 0.5$, which are the same as in Example 2; however, we assume that these speed dynamics are uncertain. Specifically, f_i and g_i are parameterized as (53) and (54), where $n_i = 2$, $\Gamma_i(s_i, R_i) = \begin{bmatrix} 0.01 |s_i| s_i & g e_3^{\mathrm{T}} R_i v_i \end{bmatrix}^{\mathrm{T}}$, and $\psi(s_i, R_i) = 1$ are known, but $\chi_{*,i} = \begin{bmatrix} -0.5 & 1 \end{bmatrix}^{\mathrm{T}}$ and $r_{*,i} = 0.5$ are unknown. Thus, $\theta_{*,i} = \chi_{*,i}/r_{*,i} = \begin{bmatrix} -1 & 2 \end{bmatrix}$ and $l_{*,i} = 1/r_{*,i} = 2$ are unknown.

To implement the projection operator used in the adaptive laws (57) and (58), we assume there exist known bounds $\underline{l}_i, \overline{l}_i \in \mathbb{R}$ such that $l_{*,i}$ is in $\underline{L}_i \triangleq \{l \in \mathbb{R} : \underline{l}_i \leq l \leq \overline{l}_i\}$. Similarly, we assume there exist

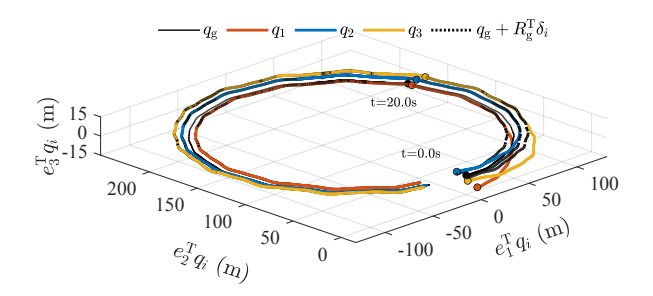


Figure 1: Agent and leader trajectories q_i and q_g .

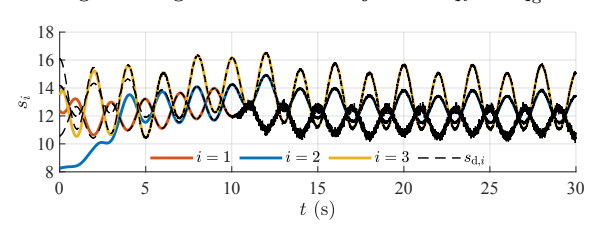


Figure 2: Agent speed s_i and desired speed $s_{d,i}$. The upper and lower speed bounds are the limits of the vertical axis.

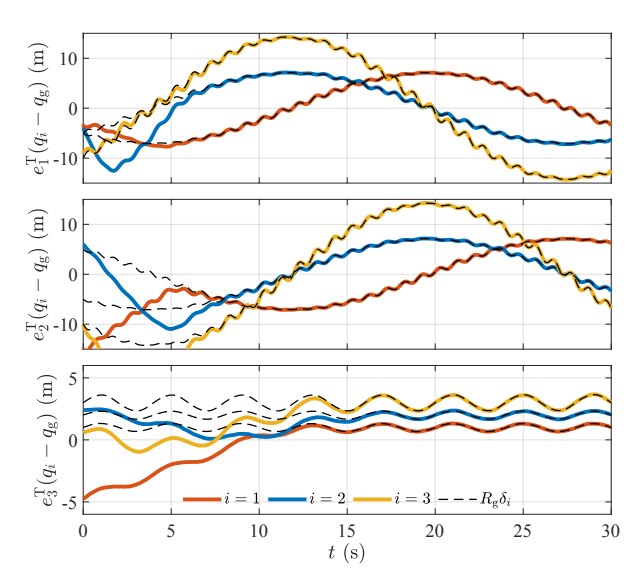


Figure 3: Agent position relative to the leader $q_i-q_{\rm g}$. Each agent achieves its desired relative position $R_{\rm g}\delta_i$ by t=20 s.

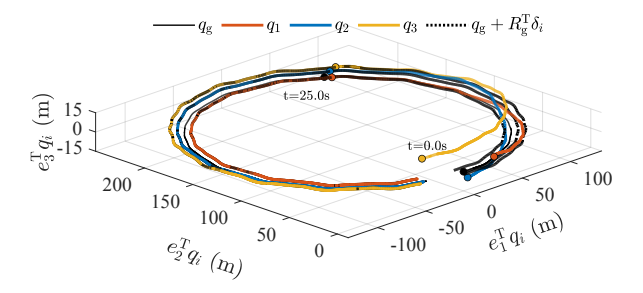


Figure 4: Agent and leader trajectories q_i and q_g .

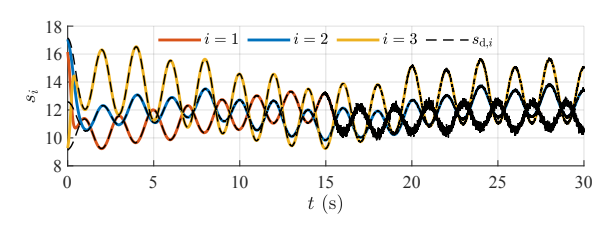


Figure 5: Agent speed s_i and desired speed $s_{d,i}$. The upper and lower speed bounds are the limits of the vertical axis.

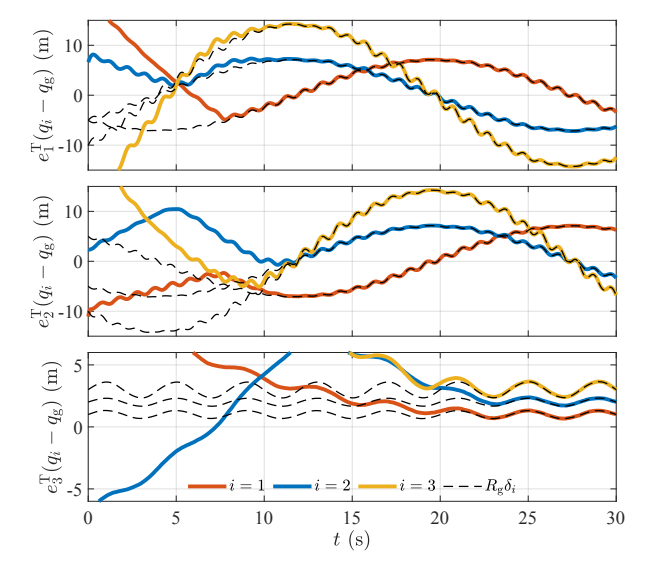


Figure 6: Agent position relative to the leader $q_i - q_g$. Each agent achieves its desired relative position $R_g \delta_i$ by t = 25 s.

known bounds $\underline{\theta}_i, \overline{\theta}_i \in \mathbb{R}^{n_i}$ such that $\theta_{*,i}$ is in $\underline{\Theta}_i \triangleq \{\theta \in \mathbb{R}^{n_i} : \underline{\theta}_i \leq \theta \leq \overline{\theta}_i$, where \leq is defined element-wise}. Next, we specify continuously differential convex functions z_i and w_i such that $L_i \triangleq \{l \in \mathbb{R} : z_i(l) \leq 0\}$ and $\underline{\Theta}_i \triangleq \{\theta \in \mathbb{R}_{n_i} : w_i(\theta) \leq 0\}$ are super sets of \underline{L}_i and $\underline{\Theta}_i$, respectively.

To develop z_i , consider $N_{l_i}: \mathbb{R} \to \mathbb{R}$ defined by

$$N_{l_i}(l_i) \triangleq \left(l_i - \frac{\bar{l}_i + \underline{l}_i}{2}\right) / \left(\frac{\bar{l}_i - \underline{l}_i}{2}\right),$$

which is a scalar normalization that maps \underline{L}_i to [-1,1], that is, $N_{l_i}(\underline{L}_i) = [-1,1]$. Then, let $z_i : \mathbb{R} \to \mathbb{R}$ be the continuously differentiable convex function defined by $z_i(l_i) \triangleq N_{l_i}^2(l_i) - 1$, and it follows that $L_i = \underline{L}_i$, which implies that $l_{*,i} \in L_i$.

To develop w_i , consider $N_{\theta_i}: \mathbb{R}^{n_i} \to \mathbb{R}^{n_i}$ defined by

$$N_{\theta_i}(\theta_i) \triangleq \left(\theta_i - \frac{\bar{\theta}_i + \underline{\theta}_i}{2}\right) \div \left(\frac{\bar{\theta}_i - \underline{\theta}_i}{2}\right),$$

where \div is element-wise vector division. Note that N_{θ_i} is a vector normalization that maps Θ_i to $[-1,1]^{n_i}$. Furthermore, we note that $\Theta_i = \{\theta \in \mathbb{R}^{n_i} : \|N_{\theta_i}(\theta)\|_{\infty}^2 - 1 \leq 0\}$; however, $\|N_{\theta_i}(\theta_i)\|_{\infty}^2 - 1$ is not continuously differentiable, and thus, it cannot be used as the function w_i . Instead, let $w_i : \mathbb{R} \to \mathbb{R}$ be the continuously differentiable convex function defined by $w_i(\theta_i) \triangleq \|N_{\theta_i}(\theta_i)\|_p^2 - n_i^{2/p}$, where $\|\cdot\|_p$ is the p-norm and p is an integer greater than 1. Thus, Θ_i is a super set of Θ_i , which implies that $\theta_{*,i} \in \Theta_i$. Furthermore, as p tends to infinity, Θ_i tends to Θ_i . In this example, we let p = 10, $l_i = 0.3$, $\bar{l}_i = 5$, $\ell_i = [-5 \quad 0.1]^T$, and $\bar{\ell}_i = [-0.1 \quad 5]^T$.

We implement the adaptive formation control (4)–(14), (16), (17), and (56)–(58), where $\varepsilon_{\rm p}=0.1,~\tau_i=0.5,~M_i={\rm diag}(2,4),~\gamma_i=10,~{\rm and}~\eta_i=0.3.$ The initial conditions $\theta_i(0)$ and $l_i(0)$ are chosen as uniform random values in the sets Θ_i and L_i . Figure 7 shows the 3-dimensional trajectories of the leader and agents, and Figure 9 shows that $q_i-q_{\rm g}$ approaches $R_{\rm g}\delta_i$, which implies that the formation control objectives are satisfied. The relative positions converge to the desired values by approximately t=25 s. The RMS of $\|\zeta_i\|$ from t=30 s to t=60 s is 0.00040 m, 0.00294 m, and 0.00165 m for agent 1, 2, and 3, respectively. Figure 8 shows that s_i approaches $s_{{\rm d},i}$, and that s_i is inside the speed bounds for all time. Figure 10 shows the adaptive parameters θ_i and l_i .

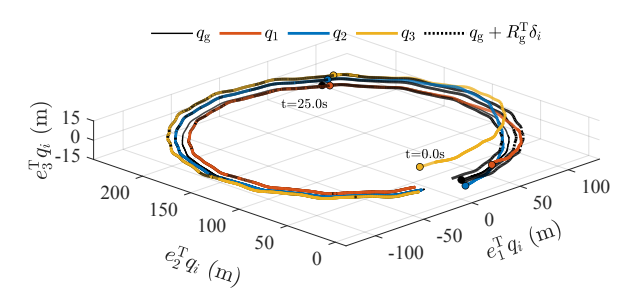


Figure 7: Agent and leader trajectories q_i and q_g .

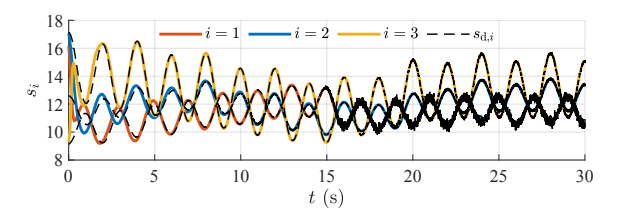


Figure 8: Agent speed s_i and desired speed $s_{d,i}$. The upper and lower speed bounds are the limits of the vertical axis.

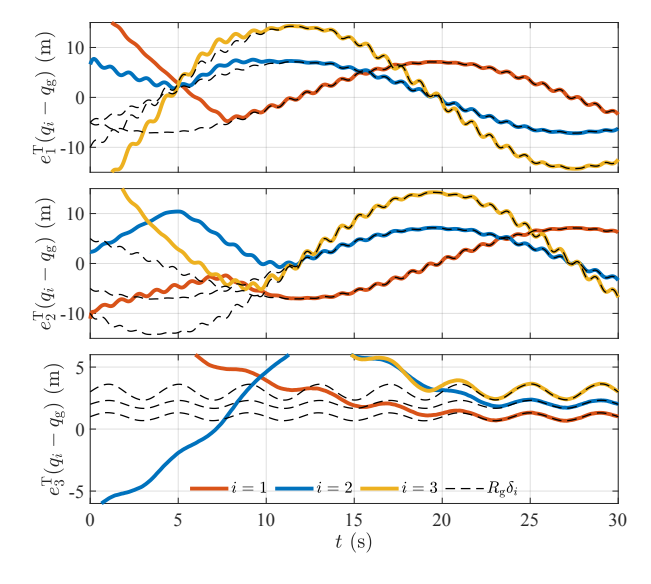


Figure 9: Agent position relative to the leader $q_i - q_g$. Each agent achieves its desired relative position $R_g \delta_i$ by t = 25 s.

The numerical examples illustrate that the formation control algorithms presented in this paper approximately achieve the objectives (O1)–(O4) in the presence of sensor noise. If the sensor noise is absent, then the RMS errors converge to zero for all examples and (O1)–(O4) are achieved as stated in Theorem 1 (non-adaptive) and Theorem 4 (adaptive).

References

- [1] B. J. Wellman and J. B. Hoagg. A flocking algorithm with individual agent destinations and without a centralized leader. *Sys. Contr. Lett.*, 102:57–67, 2017.
- [2] D. Panagou, D. M. Stipanović, and P. G. Voulgaris. Distributed coordination control for multi-robot networks using Lyapunov-like barrier functions. *IEEE Trans. Autom. Contr.*, 61(3):617–632, 2016.

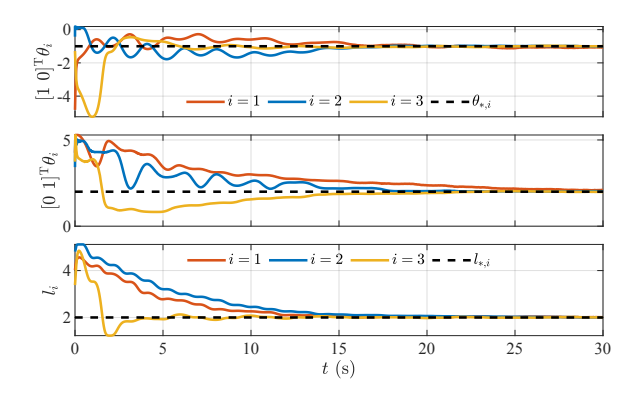


Figure 10: Adaptive parameters θ_i and l_i .

- [3] R. Olfati-Saber. Flocking for multi-agent dynamic systems: Algorithms and theory. *IEEE Trans. Autom. Contr.*, 51:401–420, 2006.
- [4] Y. Gu, B. Seanor, G. Campa, M. R. Napolitano, L. Rowe, S. Gururajan, and S. Wan. Design and flight testing evaluation of formation control laws. *IEEE Trans. Contr. Sys. Tech.*, 14:1105–1112, 2006.
- [5] G. Lafferriere, A. Williams, J. Caughman, and J. J. P. Veerman. Decentralized control of vehicle formations. Syst. Contr. Lett., 54(9):899–910, 2005.
- [6] D. Gu and Z. Wang. Leader-follower flocking: Algorithms and experiments. IEEE Trans. Contr. Sys. Tech., 17(5):1211-1219, 2009.
- [7] Y. Cao and W. Ren. Distributed coordinated tracking with reduced interaction via a variable structure approach. *IEEE Trans. Autom. Contr.*, 57(1):33–48, 2012.
- [8] J. A. Fax and R. M. Murray. Information flow and cooperative control of vehicle formations. *IEEE Trans. Autom. Contr.*, 49(9):1465–1576, 2004.
- [9] R. Olfati-Saber, J. A. Fax, and R. M. Murray. Consensus and cooperation in networked multi-agent systems. *Proc. IEEE*, 95(1):215–233, 2007.
- [10] W. Ren, R. W. Beard, and E. M. Atkins. Information consensus in multivehicle cooperative control. *IEEE Contr. Sys. Mag.*, 27(2):71–82, 2007.
- [11] W. Ren. On consensus algorithms for double-integrator dynamics. *IEEE Trans. Autom. Contr.*, 53(6):1503–1509, 2008.
- [12] Xiaowu Yang and Xiaoping Fan. Robust formation control for uncertain multiagent systems with an unknown control direction and disturbances. *IEEE Access*, 7(99):106439–106452, 2019.
- [13] M. M. Zavlanos, M. B. Egerstedt, and G. J. Pappas. Graph-theoretic connectivity control of mobile robot networks. *Proc. IEEE*, 99(9):1525–1540, 2011.
- [14] M. Guo, M. M. Zavlanos, and D. V. Dimarogonas. Controlling the relative agent motion in multi-agent formation stabilization. *IEEE Trans. Autom. Contr.*, 59(3):820–826, 2014.
- [15] C. Park, N. Cho, K. Lee, and Y. Kim. Formation flight of multiple UAVs via onboard sensor information sharing. *Sensors*, 15:17398–17419, 2015.
- [16] Weisheng Chen, Xiaobo Li, Wei Ren, and Changyun Wen. Adaptive consensus of multi-agent systems with unknown identical control directions based on a novel nussbaum-type function. *IEEE Transactions on Automatic Control*, 59(7):1887–1892, 2014.

- [17] Keum Lee and Sahjendra Singh. Variable-structure model reference adaptive formation control of spacecraft. *Journal of Guidance, Control, and Dynamics*, 35(1):104–115, 2012.
- [18] Jun Zhou, Yaohua Guo, Gongjun Li, and Jun Zhang. Event-triggered control for nonlinear uncertain second-order multi-agent formation with collision avoidance. *IEEE Access*, 7:104489–104499, 2019.
- [19] Junjie Fu, Guanghui Wen, Tingwen Huang, and Zhisheng Duan. Consensus of multi-agent systems with heterogeneous input saturation levels. *IEEE Transactions on Circuits and Systems II: Express Briefs*, 66(6):1053–1057, 2019.
- [20] Y. Cao, W. Yu, W. Ren, and G. Chen. An overview of recent progress in the study of distributed multi-agent coordination. *IEEE Trans. Industrial Informatics*, 9(1):427–438, 2013.
- [21] G. Punzo, P. Karagiannakis, D. J. Bennet, M. Macdonald, and S. Weiss. Enabling and exploiting self-similar central symmetry formations. *IEEE Trans. Aerosp. Electron. Syst.*, 50(1):689–703, 2014.
- [22] B. J. Wellman and J. B. Hoagg. Sampled-data flocking with application to unmanned rotorcraft. In *Proc. AIAA Guid. Nav. Contr. Conf.*, AIAA-2018-1856, Kissimmee, FL, January 2018.
- [23] Zhihua Qu. Cooperative control of dynamical systems: applications to autonomous vehicles. Springer Science & Business Media, 2009.
- [24] C. B. Low. A dynamic virtual structure formation control for fixed-wing UAVs. In *Proc. IEEE Int. Conf. Contr. Automation*, pages 627–632, Santiago, Chile, December 2011.
- [25] D. M. Stipanović, G. Inalhan, R. Teo, and C. J. Tomlin. Decentralized overlapping control of a formation of unmanned aerial vehicles. *Automatica*, 40(8):1285–1296, 2004.
- [26] M. Zhang and H. H. T. Liu. Formation flight of multiple fixed-wing unmanned aerial vehicles. In *Proc. Amer. Contr. Conf.*, pages 1614–1619, Washington, D.C., June 2013.
- [27] V. Darbari, S. Gupta, and O. P. Verma. Dynamic motion planning for aerial surveillance on a fixed-wing UAV. In *Proc. Int. Conf. Unmanned Aircrat Systems*, pages 488–497, Miami, FL, June 2017.
- [28] R. W. Beard, J. Ferrin, and J. Humpherys. Fixed wing UAV path following in wind with input constraints. *IEEE Transactions on Control Systems Technology*, 22(6):2103–2117, Nov 2014.
- [29] P. Panyakeow and M. Meshahi. Deconflicted algorithms for a pair of constant speed unmanned aerial vehicles. *IEEE Trans. Aerosp. Electron. Syst.*, 50(1):456–476, 2014.
- [30] T. D. Barfoot and C. M. Clark. Motion planning for formations of mobile robots. *Robotics Auton. Sys.*, 46:65–78, 2004.
- [31] C. B. Low and D. Wang. GPS-based tracking control for a car-like wheeled mobile robot with skidding and slipping. *IEEE/ASME Trans. Mechatronics*, 13(4):480–484, 2008.
- [32] C. Heintz and J. B. Hoagg. Formation control in a leader-fixed frame for agents with extended unicycle dynamics that include orientation kinematics on SO(m). In *Proc. IEEE Conf. Decision Contr.*, pages 8230–8235, 2019.
- [33] C. Heintz, S. C. Bailey, and J. B. Hoagg. Formation control of fixed-wing unmanned aircraft: Theory and experiments. In *Proc. AIAA Guid. Nav. Contr. Conf.*, AIAA-2019-1168, San Diego, CA, January 2019.
- [34] R. W. Beard, T. W. McLain, D. B. Nelson, D. Keingston, and D. Johnson. Decentralized cooperative aerial surveillance using decentralized cooperative aerial surveillance using fixed-wing miniature UAVs. *Proc. IEEE*, 94(7):1306–1324, 2006.
- [35] H. G. de Marina, Z. Sun, M. Bronz, and G. Hattenberger. Circular formation control of fixed-wing UAVs with constant speeds. In Proc. IEEE/RSJ Int. Conf. Intelligent Robots and Sys., pages 5298–5303, Vancouver, Canada, September 2017.

- [36] Sanjay P. Bhat and Dennis S. Bernstein. A topological obstruction to continuous global stabilization of rotational motion and the unwinding phenomenon. Sys. Contr. Lett., 39(1):63 70, 2000.
- [37] C. Heintz and J. B. Hoagg. Formation control for fixed-wing UAVs modeled with extended unicycle dynamics that include attitude kinematics on SO(3) and speed constraints. In *Proc. Amer. Contr. Conf.*, pages 883–888, Denver, CO, July 2020.
- [38] X. Jin. Adaptive fixed-time control for mimo nonlinear systems with asymmetric output constraints using universal barrier functions. *IEEE Trans. Autom. Contr.*, 64(7):3046–3053, 2019.
- [39] Hongwei Zhang and Frank L. Lewis. Adaptive cooperative tracking control of higher-order nonlinear systems with unknown dynamics. *Automatica*, 48(7):1432 1439, 2012.
- [40] Wenjun Song, Johan Thunberg, Xiaoming Hu, and Yiguang Hong. Distributed high-gain attitude synchronization using rotation vectors. *Journal of Systems Science and Complexity*, 28(2):289–304, Apr 2015.
- [41] M. Krstic, I. Kanellakopoulos, and P. Kokotovic. Nonlinear & Adaptive Control Design. Wiley, 1995.
- [42] E. Lavretsky and K. A. Wise. Robust and Adaptive Control with Aerospace Applications. Springer, 2013.
- [43] G. Tao. Adaptive Control Design and Analysis. Wiley, 2003.
- [44] P. Ioannou and B. Fidan. Adaptive Control Tutorial. SIAM, 2006.